

New Mexico Bureau
of
Geology and Mineral Resources

AN ISOTOPIC INVESTIGATION OF GROUND-WATER RESOURCES
IN THE OJO ALAMO SANDSTONE, SAN JUAN BASIN

by

Leslie A. Peeters

Submitted in Partial Fulfillment of
the Requirements for the Degree of
Master of Science in Hydrology

New Mexico Institute of Mining and Technology

Socorro, New Mexico

September 1983

ABSTRACT

The San Juan Basin, in northwest New Mexico, has vast reserves of strippable, low sulfur coal. Development of this resource will require large quantities of water, from an area where water sources are not abundant. Since surface-water supplies are fully allocated, increased future water demands will have to be met through ground-water development. This study concentrates on the Ojo Alamo Sandstone, the aquifer directly above the principal coal unit.

Carbon-14 and tritium methods were used to date the ground water in the Ojo Alamo Sandstone. Initial radiocarbon activities were calculated using the models of Vogel, Tamers, Pearson, Mook and Fontes. Ages from Fontes' model, ranging from modern to 26,000 years, were used for hydraulic conductivity estimates, which varied from 3×10^{-7} m/sec to 10^{-5} m/sec. Tritium analyses showed that post-bomb precipitation was present in samples with modern radiocarbon dates, indicating that active recharge is occurring.

Stable isotope results showed a clear correlation between ground-water age and stable-isotope concentrations. Samples with Pleistocene radiocarbon ages exhibited a significant depletion in deuterium and oxygen-18. This observation lends support to the hypothesis of isotopically lighter Pleistocene precipitation. Such lighter recharge

was most likely due to the combined effects of a wetter, cooler climate in the southwestern United States, with a larger percentage of winter recharge and Pacific frontal storms being the principal moisture source.

ACKNOWLEDGEMENTS

Funding for this project was provided by New Mexico Water Resources Research Institute under grant WRRRI 1345668.

The author is indebted to many people for their contributions to the project. I would like to acknowledge and thank Mr. Scott Lindsay of El Paso Natural Gas for his invaluable assistance concerning EPNG water wells and Ms. Lynn Brandvold of N.M.B.M.M.R. who performed the chemical analyses for many water samples. I am grateful to Dr. William Stone of N.M.B.M.M.R. with whom I often conferred concerning available maps, well records and publications on the San Juan Basin. In addition, I would like to thank Ms. Ingrid Klich for her field assistance, and the many landowners and residents of the study area whose hospitality and cooperation made the winter of 1982-83 rewarding. Sincere appreciation is extended to Mr. Mike Tansey for sharing his knowledge of isotope hydrology. I also thank the many students and secretaries of N.M.I.M.T. who have provided constant humor and encouragement over the past two years.

I extend a special thanks to my advisor, Dr. Fred Phillips, who not only suggested the thesis problem but provided continual guidance and advice through out the study, in addition to critically reviewing this manuscript. Finally, I would like to thank the members of my family whose support and encouragement have made my education possible.

TABLE OF CONTENTS

	Page
PROBLEM AND PURPOSE	1
INTRODUCTION	
Location and Access	4
Duration of Study	4
Climate	6
Drainage	7
Landforms	8
Vegetation	8
Land Ownership and Use	9
Sample Locations and Numbering System	10
Units of Measurement	13
PREVIOUS INVESTIGATIONS	14
GEOLOGY	
Regional Setting	16
Stratigraphy and Hydrologic Properties	
Fruitland Formation	18
Kirtland Shale	19
Ojo Alamo Sandstone	21
Nacimiento Formation	23
San Jose Formation	25
METHODS	
Stable Isotopes	28
Carbon-14	32
Tritium	41
Noble Gases	43
HYDRAULICS OF THE OJO ALAMO SANDSTONE	46
MODELS	
Vogel	56
Tamers	56
Pearson	57
Mook	59
Fontes	60

Table of Contents continued

Page

RESULTS

Stable Isotopes	63
Carbon-14	63
Tritium	75
Noble Gases	79

INTERPRETATIONS

Stable Isotopes	80
Carbon-14	85
Tritium	87

SUMMARY	91
---------------	----

SIGNIFICANCE AND RECOMMENDATIONS	93
--	----

REFERENCES	95
------------------	----

APPENDIX I	103
------------------	-----

APPENDIX II	104
-------------------	-----

LIST OF FIGURES

	Page
Figure 1. Location map for study area	5
Figure 2. Outcrop of Ojo Alamo Sandstone and sample locations	11
Figure 3. Well numbering system	11a
Figure 4. Structural elements of the San Juan Basin	17
Figure 5. Potentiometric surface map for the Ojo Alamo Sandstone	47
Figure 6. Potentiometric surface map for the Nacimiento Formation	48
Figure 7. Generalized flow paths for the Ojo Alamo Sandstone	49
Figure 8. Vertical head gradient map between the Nacimiento Formation and Ojo Alamo Sandstone	51
Figure 9. Vertical head gradient map between the Ojo Alamo and Pictured Cliffs Sandstones	52
Figure 10. Map of $\Delta D / \Delta^{18}O$	65
Figure 11. Graph of ΔD vs. $\Delta^{18}O$	66
Figure 12. Isochron map of Ojo Alamo Sandstone	76
Figure 13. ΔD vs. ^{14}C age	82
Figure 14. Graph of sulfate vs. chloride	86
Figure 15. Map of hydraulic conductivities	88
Figure 16. Tritium concentration vs. Carbon-14 age	89

LIST OF TABLES

	Page
Table 1. Sample number, name and location	12
Table 2. Isotopic enrichment of deuterium and ^{18}O	64
Table 3. ^{14}C activity and ^{13}C enrichment	67
Table 4. Chemical analyses for water samples	69
Table 5. Major ion concentrations in meq/l	70
Table 6. ^{14}C initial activities	71
Table 7. ^{14}C ages	73
Table 8. Sensitivity analysis for ^{14}C models	77
Table 9. Tritium concentrations	78

PROBLEM AND PURPOSE

The San Juan Basin is an energy-resource-rich area of the southwest. Among the most important resources is coal, with reserves estimated at 175 billion metric tons (Shomaker et al., 1971; Kottowski, 1975). The Fruitland Formation alone may have as much as 136 billion metric tons (150 billion tons). Strippable reserves, those overlain by less than 76 meters (250 feet) of overburden, occur primarily in the Fruitland Formation and have been estimated at 6.1 billion metric tons (Coal Group, N.M.B.M.M.R., written communication). Development of these vast reserves has, up to now, only extracted a small portion of the available coal. Development is accelerating and is expected to reach 30 to 40 million tons/year for the strippable reserves in the Fruitland Formation alone (Shomaker and Stone, 1976).

With increased coal development will come an increased demand for water. Strip mining of coal requires large quantities of water. It is primarily used for irrigation of reclaimed land, dust control and coal washing. In addition, the electric-power generating plants using the mined coal require water for boiler feed and cooling fluid. The population increase due to industrialization will also add to the water supply demand. Future coal development depends

heavily on the availability of water.

Presently, the major source of water for the more populated areas of the San Juan Basin is the San Juan River and its tributaries. Cooper and Trauger (1967) report that ground water contributes less than 1% of the annual water consumption. Shomaker and Stone (1976) give several reasons for this: surface water is readily available, ground water is often deep and saline, and little is known of the occurrence and availability of suitable supplies. However, surface water in northwestern New Mexico has been fully allocated, leaving ground water as the major source for additional demands.

As Shomaker and Stone (1976) point out, little is known of the occurrence and availability of suitable ground water supplies. If the aquifers of the San Juan Basin are to be developed effectively, efficiently, and with foresight, information regarding the hydraulic properties of the aquifers is needed. In-depth hydrologic studies of the area are necessary for a rational management of the ground-water resources in the basin.

The purpose of this investigation is to provide detailed hydrologic information concerning the Ojo Alamo Sandstone through the use of isotopic methods. Techniques employed are tritium, ^{14}C , ^{18}O and deuterium, and noble-gas

concentrations. The specific objectives are:

- 1) to date the ground water of the Ojo Alamo Sandstone in the San Juan Basin, and from the data estimate aquifer parameters pertinent to ground-water development.

- 2) to obtain isotopic data which will elucidate the nature of Pleistocene climatic changes in north-western New Mexico.

INTRODUCTION

Location and Access

The study area is located in parts of San Juan, Rio Arriba, Sandoval and McKinley Counties, New Mexico (Figure 1). Field work was concentrated in the area bounded by Highway 44 and the outcrop of the Ojo Alamo Sandstone, although five sample locations are to the northeast of the highway. Population centers include Lybrook, Nageezi and Dzilh-Na-O-Dith-Hle.

Highway 44 is a major paved road within the study area. All sample sites can be reached by using the countless oil and gas company roads stemming from Highway 44. These roads are not paved and become virtually impassable during the wet seasons owing to the shaly nature of many geologic units.

Duration of Study

Field work was conducted from November 1982 through March 1983. Compilation of field data and laboratory analyses took place during the spring and early summer of 1983.

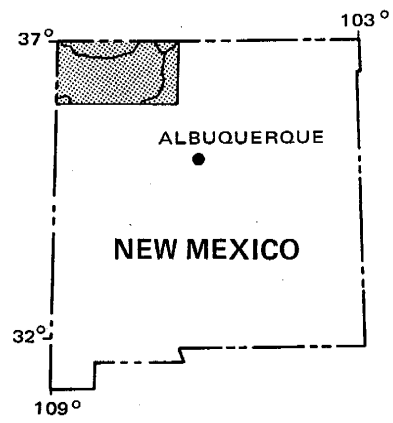
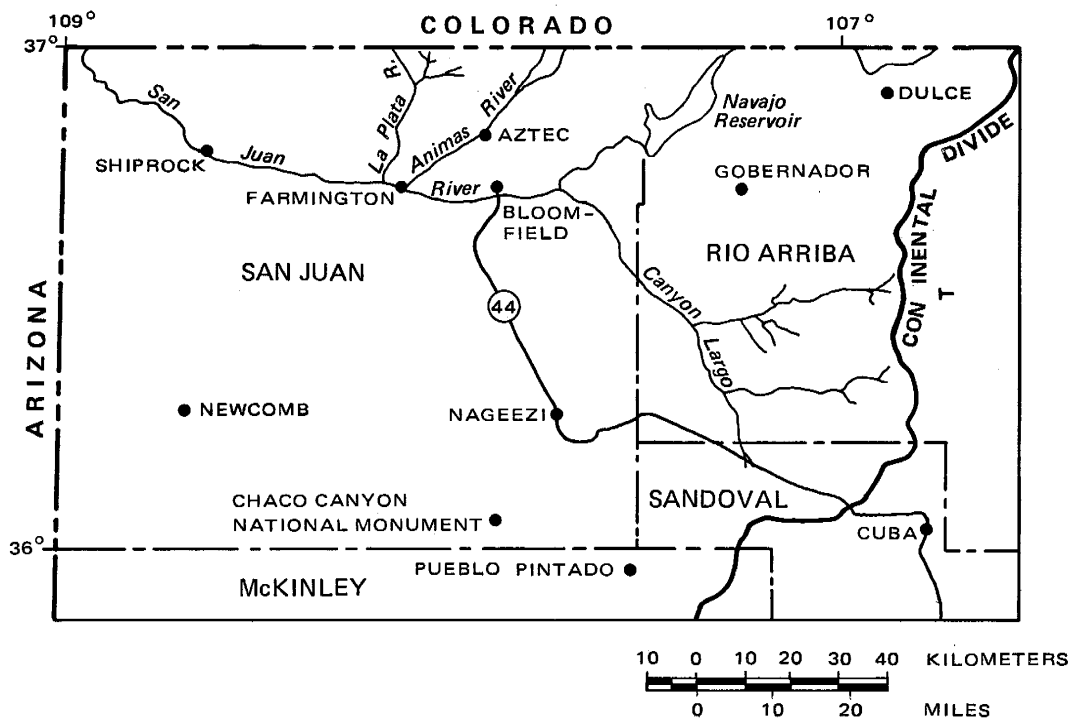


Figure 1. Location map for study area.

Climate

The climate of the San Juan Basin is arid to semi-arid. It is characterized by abundant sunshine, low relative humidity and large temperature contrasts. The study area receives an average of 21.3 cm (8.4 in) precipitation annually except near Cuba where 33.2 cm (13.1 in) is the annual average. Precipitation in northwestern New Mexico has two principal sources. Summer moisture primarily comes from the Gulf of Mexico while winter precipitation originates in the Pacific Ocean. As much as 65% of the total annual rainfall occurs during intense summer (July through September) thunderstorms, and therefore much is lost to runoff (Craig, 1980).

The U.S. Weather Service maintains weather stations at Bloomfield (northern edge of study area), Chaco Canyon National Monument (11 km southwest of central portion of study area) and Cuba (southern extent of study area) (Figure 1). The respective mean annual temperatures are 11.6 °C, 9.5 °C and 7.9 °C. Mean summer maximums are 32.4 °C, 31.1 °C and 29.4 °C while mean winter minimums are -6.9 °C, -10.2 °C and -11.4 °C, respectively.

Drainage

The north-trending Continental Divide lies along the east side of the San Juan Basin (Fassett and Hinds, 1971). Approximately 4/5 of the study area is to the west of the divide, in the San Juan River drainage basin. The two major tributaries of the San Juan River, the Animas and La Plata Rivers, originate in Colorado and flow south to join the San Juan in New Mexico. Besides these two perennial rivers, numerous intermittent streams flow north through the central part of the basin. The most significant of these are the Chaco River and Canyon Largo. The Chaco River drains southern and western parts of the basin and enters the San Juan River from the south, near the town of Shiprock. Canyon Largo heads at the Continental Divide and flows northwesterly to join the San Juan River at Blanco, New Mexico.

The small portion of the study area located to the east of the Continental Divide is drained by ephemeral streams in the Rio Grande watershed. The Rio Puerco is the master stream for this drainage area but is intermittent south of Cuba. The Rio Puerco flows south until it merges with the Rio Grande, approximately 81 km (50 miles) south of Albuquerque.

Landforms

Cooper and Trauger (1967) describe the area south of the San Juan River as a "gently northward-sloping, desolate, and rather featureless plain, cut by numerous arroyos and with only an occasional lone butte or mesa to provide contrast". The study area, forming a narrow band in the center of the basin, is best described as a gently sloping plateau with locally prominent sandstone mesas and cliffs. The major streams have cut deeply into the alluvium and underlying rock units, forming steep walled arroyos where sandstones are present.

The elevation of the area under investigation ranges from 1850 m (6070 ft) near Farmington to 2267 m (7438 ft) just west of Cuba. The most prominent mesa, Huerfano Mountain, rises 200 meters (656 ft) above the surrounding countryside.

Vegetation

Life zones in the San Juan River Basin range from upper Sonoran to Canadian (Bailey, 1913), with the former being characteristic of the study area. Grass and sage brush dominate the landscape of the central basin. At the higher elevations pinon and juniper are present. South of Bloomfield, the Navajo Indian Irrigation Project (NIIP) is

currently irrigating 18,200 hectares (45,000 acres) of land. Eventually, a total of 44,775 hectares (110,640 acres) will be irrigated as part of NIIP (Al Keller, Farmington BIA, oral communication).

Land Ownership and Use

The federal government is the largest land owner in the study area. Administered by the Bureau of Land Management (BLM), approximately 75% of the land is leased out for cattle and sheep grazing. The northern and central portions of the study area are in what is commonly referred to as the checkerboard area. The land ownership of this area gives a checkerboard appearance with the Navajo tribe and the federal government owning alternating sections of land. Scattered throughout the area are sections owned by the State of New Mexico, but these do not number more than 35. Private ownership is even sparser, with most sections occurring along Highway 44 or near Cuba.

The land is primarily used for stock grazing. Natural gas is also an important aspect of the area as is evidenced by the ubiquitous natural gas wells. Just south of Bloomfield and west of Highway 44 is the Navajo Indian Irrigation Project where 18,200 hectares (45,000 acres) are currently being irrigated.

Sample Locations and Numbering System

Prior to field work, all wells and springs tapping the Ojo Alamo Sandstone were located and plotted on five 1:100,000 metric scale topographic maps (Farmington, Navajo Reservoir, Chaco Canyon, Chaco Mesa, Abuqui). Well locations were obtained from Stone et al. (1983).

Eighteen suitable sample sites were found in the study area (Figure 2). Virtually all operative and accessible wells (electric and windmills) tapping the Ojo Alamo Sandstone were sampled. Ojo Alamo Springs with biological activity were not sampled due to carbon-14 restrictions, nor were those with obscure discharge points or inaccessible locations.

The location of a water well or spring is designated by a series of numbers that represent a geographic description based on the Federal system of land subdivision. The four parts of the location number refer to the township, range, section, and tract within a section, respectively (Figure 3). Since all wells and springs are located north of the New Mexico base line and west of the New Mexico principal meridian, the N and W (designating north and west) have been omitted from the location numbers in this report. Table 1 lists the project sample number, well or spring name, and location number.

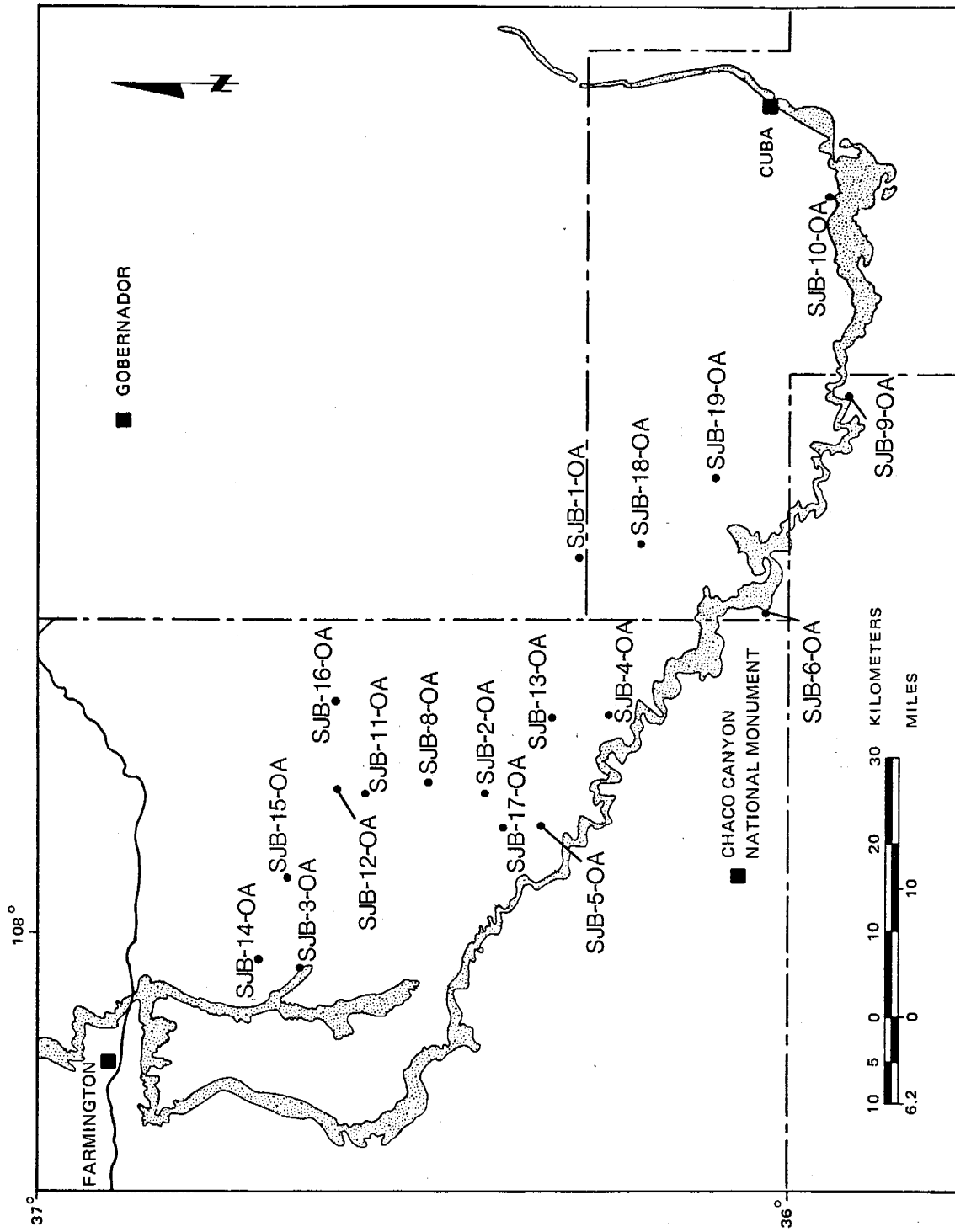
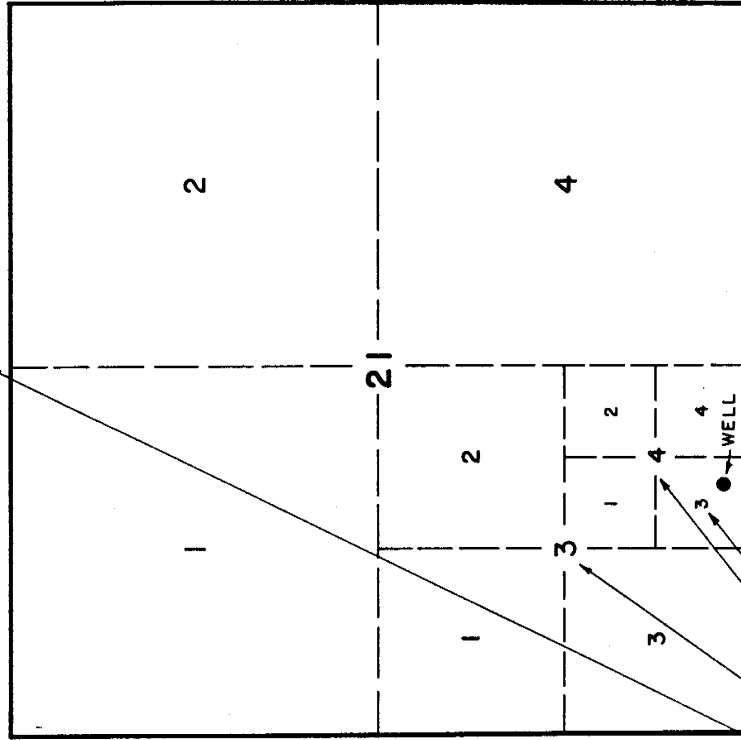


Figure 2. Outcrop of the Ojo Alamo Sandstone and sample locations.

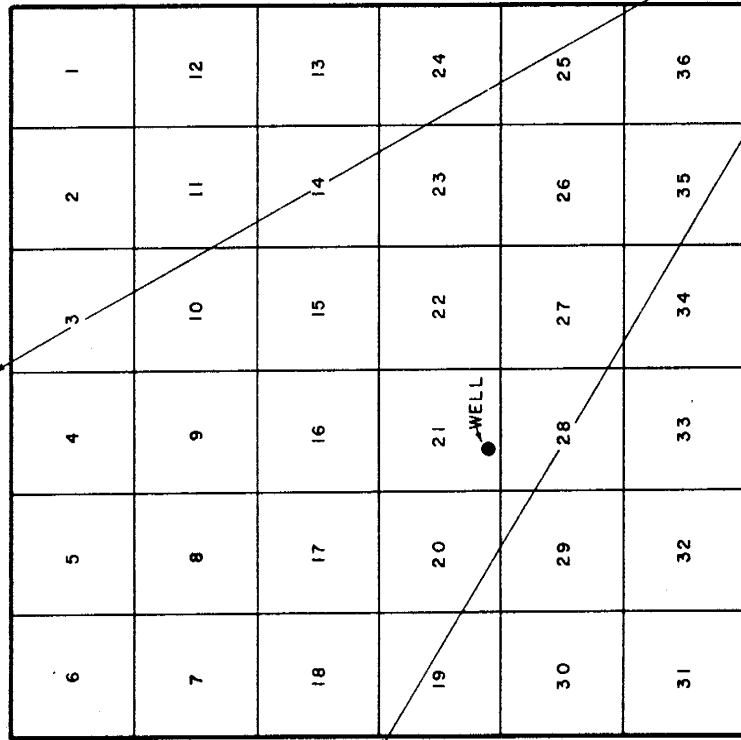
TRACTS WITHIN A SECTION

SECTION 21



SECTIONS WITHIN A TOWNSHIP

R 2 E



T 22 S

WELL 22S. 2E. 21.3 4 3

Sample #	Name	Location
SJB-01-OA	Lybrook	23.07.14.1
SJB-02-OA	B of C Mission	24.10.12.2223
SJB-03-OA	Pete Spring	27.12.35.4244
SJB-04-OA	Powerline WM	23.09.25.3131
SJB-05-OA	Kimbeto WM	24.10.33.4441
SJB-06-OA	Ojo Socorro	21.07.19.4441
SJB-08-OA	Dzilth	25.09.19.1111
SJB-09-OA	Ojo Encino	20.05.22.4422
SJB-10-OA	Johnsons TP	20.02.19.124
SJB-11-OA	Huerfano #2	26.10.25.4141
SJB-12-OA	Huerfano #1	26.10.13.423
SJB-13-OA	Nageezi CH	23.09.01.1141
SJB-14-OA	Chaco Camp #9	27.12.13.142
SJB-15-OA	Hilltop	27.11.26.4111
SJB-16-OA	Kah-Des-Pah	26.08.18.3114
SJB-17-OA	Tsah Tah	24.10.15.114
SJB-18-OA	Sisnathyel	22.07.01.4442
SJB-19-OA	Chimney Dam	21.06.03.2212

Table 1. Sample number, name and location.

Units of Measurement

In this report, all quantitative information is expressed in metric units. In most cases, the English equivalent follows in parentheses. Appendix I lists useful conversion factors. Large figures are rounded off.

PREVIOUS INVESTIGATIONS

The geology of the Upper Cretaceous and Tertiary rocks of the San Juan Basin has been studied by several authors. An early publication by Sinclair and Granger (1914) dealt with the Paleocene deposits in the basin. Reeside (1924) investigated the Upper Cretaceous and Tertiary formations along the western side. In the eastern part of the basin the Eocene, Paleocene and oldest Cretaceous formations were studied by Dane (1946). Baltz (1967) published a study of the Upper Cretaceous and Tertiary rocks in the southern half of the Jicarilla Apache Indian Reservation. Fassett and Hinds (1971) conducted a basin wide study on the geology and fuel resources of the Fruitland Formation and Kirtland Shale.

Isolated sections of the current study area have been included in several ground-water investigations. Renick (1931) conducted a preliminary survey on the ground-water resources of western Sandoval County. A reconnaissance investigation by Rapp (1959) concentrated on an area near Farmington. Cooley et al. (1969) studied the regional hydrology of the Navajo and Hopi Indian Reservations. The southern portion of the study area was included in an assessment of the ground-water resources of the Jicarilla Apache Indian Reservation by Baltz and West (1967). The southern margin of the basin was the location for a ground-

water study by Cooper and John (1968). Brown (1976), Anderholm (1979) and Craigg (1980) investigated the hydrogeology of 15-minute-quadrangles near Aztec, Cuba and Chaco Canyon National Monument, respectively.

The question of the availability of water for energy development has usually been the impetus behind most of the recent ground-water investigations in the San Juan Basin. Brimhall (1973) discussed the ground-water hydrology of the Tertiary sediments. Shomaker and Stone (1976) concentrated on aquifers below the Fruitland coal beds in their investigation of water availability for coal development. Lyford (1979) dealt with all of the principal aquifers in the basin in his brief study, but treated the Tertiary units as one aquifer. Most recently, Stone et al. (1983) published a comprehensive overview on the hydrology of the San Juan Basin.

GEOLOGY

Regional Setting

The San Juan Basin is a structural depression in northwestern New Mexico and southwestern Colorado that contains sedimentary rock units ranging in age from Cambrian to Quaternary. Covering approximately 77,000 km² (30,000 mi², Craig, 1980, p.27) it is bounded on the north by the San Juan Mountains, on the west by the Defiance Uplift, on the south by the Zuni Mountains, and on the east by the Nacimiento Uplift (Kelley, 1950, p.101) (Figure 4). Nearly circular in plan view, it is asymmetrical in section with a maximum stratigraphic thickness of almost 4,400 m (14,423 ft) near Navajo Reservoir (Lyford, 1979). Sedimentary rocks of Jurassic and Cretaceous age crop out along the basin margins with Tertiary sediments making up the central basin. Quaternary deposits are restricted mainly to major valleys (Stone et al., 1983, p.11).

Kelley (1950, p.103) first named and described the different structural elements of the San Juan Basin. The study area lies entirely within the Central Basin structural element which is bounded on the west, north and east by the abrupt Hogback Monocline. The gently, northeasterly dipping Chaco Slope is the southern boundary of the Central Basin (Figure 4).

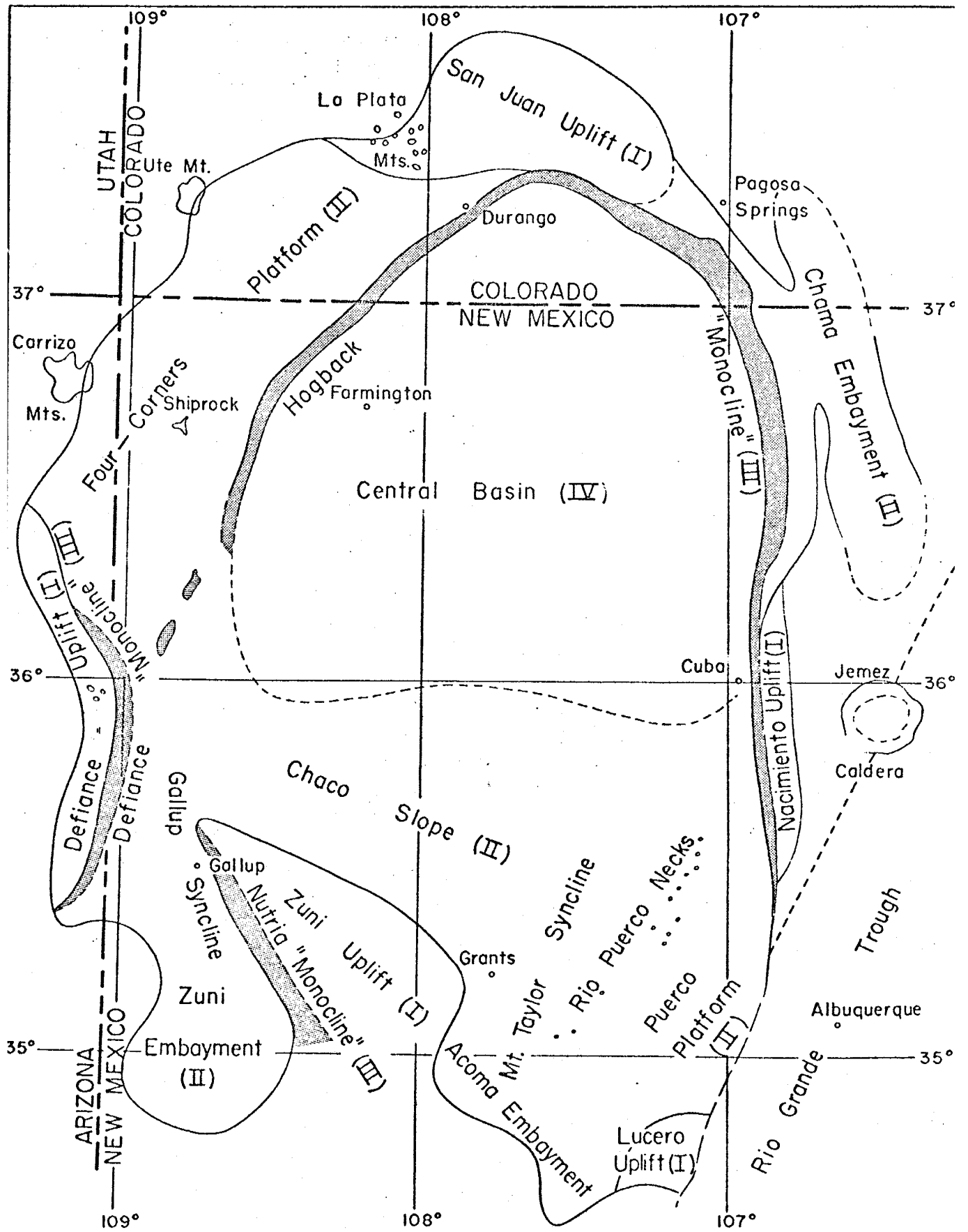


Figure 4. STRUCTURAL ELEMENTS OF THE SAN JUAN BASIN (from Ke11 1950)

Stratigraphy and Hydrologic Properties

Fassett and Hinds (1971) discussed in depth the geology of the Fruitland Formation and Kirtland Shale. Much of the following discussion pertaining to these two formations is taken from their work.

Fruitland Formation: The Fruitland Formation was named by Bauer (1916) for the outcrops exposed along the San Juan River near Fruitland, New Mexico. It is composed of interbedded sandstone, siltstone, shale, carbonaceous shale, and coal. All rock units are discontinuous but the coal beds are locally persistent, being traceable for several miles. Of Upper Cretaceous age, it represents the establishment of a continental environment as the epeiric sea made its final retreat.

The Fruitland Formation lies conformably on the Pictured Cliffs Sandstone. The thickness ranges from 0 to approximately 150 m (492 ft) and is locally variable due to an indefinite upper contact. The average thickness is 91 to 107 m (300 to 350 ft).

When considered as aquifers, the Fruitland Formation and Kirtland Shale are most often classified as undivided. Based on their similar hydrologic properties, this classification will be used in discussing the aquifer

characteristics and these characteristics will be dealt with in the section pertaining to the Kirtland Shale.

Kirtland Shale: Defined by Bauer (1916, p.274) the Kirtland Shale was named for the town of Kirtland, New Mexico on the San Juan River. Bauer described the Kirtland Shale as having three parts: "a lower shale 271 feet thick, a sandy part, here named the Farmington Sandstone Member..., and an upper shale 110 feet thick." Fassett and Hinds (1971, p.23) considered the Kirtland Shale to have two members: the lower shale member of Bauer and the undivided Farmington Sandstone Member and upper shale member of Bauer. They described the lower shale as a predominantly gray shale with thin interbeds of siltstone and sandstone. The latter member is composed of a series of interbedded sandstone lenses and shale. The shale near the top of the Kirtland has characteristic purple, green, white or gray coloring. Upper Cretaceous in age, the Kirtland Shale was deposited in an environment similar to that of the Fruitland. The lack of coal in the Kirtland suggests that swamps were relatively scarce, probably due to better drainage networks (Fassett and Hinds, 1971, p.25).

The lower contact of the Kirtland Shale is placed just above the highest coal bed or carbonaceous shale bed. Due to a complex stratigraphic relationship and a commonly

obscure contact the Fruitland Formation and Kirtland Shale are often mapped as "undivided". In the eastern part of the Central Basin the Kirtland Shale is missing in the subsurface due, in most part, to erosion or lack of deposition. The Kirtland Shale increases in thickness from 0 m in the east to approximately 610 m (2000 ft) near Farmington.

The Fruitland Formation/Kirtland Shale interval is of little importance as an aquifer. The interbedded sandstones may yield small quantities of water but it is probably of high salinity. Electric logs of gas wells indicate that the sandstone beds of the Fruitland Formation are thin, of low porosity, and contain water of poor quality (Brown, 1976, p.54). Baltz and West (1967, p.H17) reported that deep oil and gas wells have produced highly saline water and natural gas from the Fruitland and Kirtland.

Stone et al. (1983, p.21) summarized the hydrologic properties and water quality of the Fruitland Formation/Kirtland Shale. Based on tests performed by the U.S. Geological Survey on the coal beds and associated sediments, expected transmissivities range from .9 to .93 m^2/day (1 to 10 ft^2/day). Specific conductance is typically higher than 5000 usiemens/cm but may be lower in some areas. Stock wells discharge generally less than 55 m^3/day (10 gpm)

Ojo Alamo Sandstone: Originally named by Brown (1910), the Ojo Alamo Sandstone has had a rather complicated and confusing nomenclatural history. Over a span of 63 years, seven definitions have been proposed, yet there is still no consensus. Fassett (1973) discussed at length the evolution of the definition of the Ojo Alamo Sandstone. Baltz (1967, p.31) described the rocks that lie above the Kirtland Shale as a persistent fine- to coarse-grained locally conglomeratic sandstone with lenses of olive-green to gray shale. Brimhall (1973) described two types of deposits for the Ojo Alamo Sandstone. The first is a floodplain deposit consisting of broad sandstone units that persist laterally for several miles. Channel deposits, the second type, are thick but usually less than one mile wide. The floodplain deposits are fine- to medium-grained sandstone, while the channel deposits are medium- to coarse-grained sandstone.

The Ojo Alamo Sandstone crops out in a narrow arcuate band extending from Cuba to Farmington (Figure 2). It dips to the northeast and reaches a maximum depth of 1,111 m (3,645 ft) in the basin center (Stone et al., 1983, p.20). The base of the Ojo Alamo Sandstone rests with erosional unconformity on the Kirtland Shale and evidence of scouring and deep channeling can be seen in many places (Baltz, 1967, p.33). The thickness of the unit is variable due to the very irregular basal contact, but ranges from 22 to 95 m (72

to 313 ft).

Brimhall (1973) stated that "the Ojo Alamo Sandstone is a major source of supply of ground water in the San Juan Basin." As a result of over- and underlying siltstones and shales, the Ojo Alamo is an artesian aquifer. One flowing well (SJB-16-OA) was observed in the study area. The channel deposits have the best potential for supplying large quantities of water due to their thickness and grain size, but may be difficult to locate (Brimhall, 1973).

The quality of the water in the Ojo Alamo varies across the basin. South and east of Farmington, wells open to the Ojo Alamo produce water in quantities sufficient for domestic and stock needs but total dissolved solids (TDS) typically exceed 1000 mg/l with high sulfate concentrations (Rapp, 1959). Brimhall (1973) reported relatively low TDS values for the Ojo Alamo, ranging from 360 mg/l to 824 mg/l. As a rule of thumb for field work, TDS can be estimated by multiplying a measured specific conductance by .62. Table 4 lists specific conductance (i.e., electrical conductance) values measured by the authors for wells and springs in the study area. They closely agree with those reported by Brimhall.

Brimhall (1973) summarized pumping test data for six wells tapping the Ojo Alamo Sandstone. Transmissivities were determined to vary from 5 to 15 m²/day (57 to 164 ft²/day). Yields ranged from 191 to 981 m³/day (35 to 180 gpm) although these are not necessarily maximum values. Storage coefficients ranged from 2 x 10⁻⁴ to 6.7 x 10⁻³.

Nacimiento Formation: Keyes (1906) named and defined the Nacimiento Formation for exposures near Cuba, New Mexico. It consists of shale and interbedded soft to resistant sandstone. Baltz and West (1967, p.H20) described the Nacimiento Formation as consisting mainly of clay, shale, siltstone and soft sandstone in the southern part of their study area (southeast corner of the Central Basin) while in the northern portion (east central part of the Central Basin) as much as 50% of the formation is sandstone. They noted however, that the "lateral change in facies is so gradual and exposures are so discontinuous on the east side of the area that it is impossible to map any logical lithologic boundary between facies". The Paleocene Nacimiento Formation is considered fluvial in origin (McDonald, 1972), containing the irregular, coarse, channel sandstones and the floodplain silts and clays of the fluvial environment (Brown, 1976, p.42).

Fassett and Hinds (1971, p.39) indicated that throughout most of the basin the Nacimiento Formation conformably overlies the Ojo Alamo Sandstone. The contact is gradational and Baltz (1967, p.41) reported that in his area of investigation it occurred over a span of a few inches to several feet of sandy shale. Evidence of intertonguing can be seen in outcrops in the southwestern part of the basin (Baltz et al., 1966) and near Farmington (O'Sullivan and Beikman, 1963). Just south of the New Mexico - Colorado border and west of the La Plata River, the Nacimiento is in direct contact with the Kirtland Shale. The thickness of the Nacimiento Formation varies owing to an erosional contact with the overlying San Jose Formation but generally the unit thickens northward (Baltz and West, 1967, p.H20). Stone et al. (1983, p.19) reported the thickness to be 127 to 680 m (418 to 2,232 ft).

Limited quantities of water may be obtained from localized artesian aquifers in the sandstone horizons of the Nacimiento Formation. The Nacimiento Formation as a whole however, cannot be considered an aquifer according to Brimhall (1973). Baltz and West (1967, p.H21) pointed out that the water bearing properties of the Nacimiento Formation vary from south to north because of the lithologic change from a predominantly shale facies in the south to one of thick sandstone with interbedded shales in the north.

Brimhall (1973) reported a flowing well in eastern Rio Arriba County along Canyon Largo that produced water from a sandstone aquifer in the Nacimiento Formation. El Paso Natural Gas Company reported yields from 1 to 6 m³/day (16 to 100 gpm) in nine water wells producing from the Nacimiento near Aztec (Brown, 1976, p.44). Brimhall (1973) concluded that wells may yield from 191 m³/day (35 gpm) to over 1,090 m³/day (200 gpm). Stone et al. (1983, p.19) suggested that transmissivities may be as high as 9 m²/day (100 ft²/day) based on tests of similar aquifers. Specific conductance of the water in the Nacimiento ranges from less than 1500 usiemens/cm in some of the more extensive sandstones to greater than 4000 usiemens/cm near the San Juan River. Brown (1976, p.44) measured the specific conductance in six Nacimiento wells near Aztec. The average was 2000 usiemens/cm. It seems then, that the Nacimiento Formation is of little significance as an aquifer near its southern boundary but may be of local importance towards the north or where coarse, extensive sandstones exist.

San Jose Formation: Simpson (1948) named the San Jose Formation for exposures along the San Jose Valley in northwest Sandoval County, New Mexico. In their investigation of the ground-water resources of the Jicarilla Apache Indian Reservation, Baltz and West (1967) defined four intricately related members of the San Jose Formation.

In ascending order, they are the Cuba Mesa Member, the Regina Member, the Llaves Member and the Tapicitos Member. The Cuba Mesa and Llaves Members are primarily coarse-grained sandstones while the Regina and Tapicitos Members are shales with interbedded sandstone (Baltz, 1967, p.45). For a detailed description of each member refer to Baltz and West (1967). Anderholm (1979, p.33) reported that all previous investigators have interpreted the San Jose Formation to be fluvial deposits of Eocene age.

The San Jose Formation makes up most of the surface of the Central Basin. Its total thickness ranges from less than 61 m (200 ft) in the west and south to almost 823 m (2700 ft) in the basin center between Cuba and Gobernador (Stone et al., 1983, p.18). Throughout most of the basin the San Jose unconformably rests upon the Nacimiento Formation but a few miles northeast of Cuba, the San Jose is in unconformable contact with the Lewis Shale (Baltz, 1967, p.42).

Cooper and Trauger (1967) stated that in the eastern part of the basin the Nacimiento and San Jose Formations together "should be considered an important potential reservoir of large volume." Brimhall (1973) reported that wells may yield 164 to 327 m³/day (30 to 60 gpm) from the Cuba Mesa Member. However, Baltz and West (1967, p.65)

calculated that a well tapping all the beds of sandstone in the San Jose Formation might yield 7,850 m³/day (1,440 gpm). Stone et al. (1983, p.18) reported transmissivities of 4 and 11 m²/day (40 and 120 ft²/day) for two wells penetrating only 30.5 m (100 ft) of formation in southwestern Rio Arriba County. The average specific conductance of water from the sandstone aquifers is about 2000 usiemens/cm. Though the San Jose Formation may have the potential for yielding large quantities of water, it may not always contain water suitable for domestic use. For example, the municipal water supply for Cuba is obtained from the Cuba Mesa Member of the San Jose Formation. An analysis of the water indicated a TDS of only 566 mg/l but high concentrations of sulfate, sulfide and magnesium render the water undesirable for human consumption (Anderholm, 1979, p.74). Most inhabitants of Cuba obtain their drinking water from mountain springs.

METHODS

Stable Isotopes

Theory: The stable isotopic composition of a ground-water sample can give valuable information concerning the origin and history of a water reservoir (Fontes, 1980). If the isotopic composition of the discharging ground water has not been altered along its flow path, clues to its origin (i.e. source, elevation, type of recharge) may be available. But this implies that deuterium and oxygen-18 are conservative tracers, which is not always the case (Fontes, 1980). However, modification of the initial isotopic composition can also be helpful, in that it reflects the history (i.e. mixing, high temperature exchange, membrane filtration) of ground-water flow.

Craig (1961b) analyzed 400 worldwide meteoric water samples for deuterium and oxygen-18 enrichments relative to "standard mean ocean water" (SMOW). He found that the deuterium and oxygen-18 concentrations were linearly related, with the exception of those samples from closed basins. The equation of the line relating the two heavy isotopes is

$$\delta D = 8\delta^{18}O + 10$$

and is referred to as the Meteoric Water Line (MWL). However, this line does not pass through the point representing the composition of ocean water (i.e., the origin) thus suggesting that evaporation from the ocean does not produce vapor which is in isotopic equilibrium with it. Water which has undergone secondary evaporation (primary evaporation being evaporation from the ocean surface) will plot on a line with a slope ranging from 3 to 5 (Craig, 1961b), depending on the rate of evaporation. This characteristic slope "fingerprints" water which has been enriched due to partial evaporation.

Dansgaard (1964) found that oxygen-18 and deuterium concentrations in precipitation are temperature dependent. He determined that a linear relationship exists between the ^{18}O values of average annual precipitation and the average annual air temperature. This relationship can be expressed by the equation:

$$\delta^{18}\text{O} = 0.695T - 13.6$$

where $\delta^{18}\text{O}$ is the mean annual $\delta^{18}\text{O}$ and T is the average annual temperature in $^{\circ}\text{C}$. This temperature dependence manifests itself in several recognized "effects". Briefly, they are:

- latitude effect: the heavy isotope concentration of precipitation decreases with increasing latitude.

- elevation effect: an increase in elevation results in a decrease in deuterium and oxygen-18.
- seasonality: summer precipitation has higher heavy isotop concentrations than winter precipitation.

The evaporation process also causes several general trends. Two important ones are the amount effect and the origin effect. The amount effect (or the humidity effect) is especially important in arid or semi-arid climates. A negative correlation exists between the amount of precipitation and the oxygen-18 content of the precipitation. The reason for this is the inverse relationship between the enrichment of heavy isotopes due to evaporation and the relative humidity (i.e., low humidity results in high enrichment and high humidity will allow little enrichment).

The origin effect arises from the fact that though the major oceans are of relatively stable isotopic composition (Epstein and Mayeda, 1953), local sources of moisture may be either enriched or depleted in heavy isotopes with respect to sea water. For example, the humidity over the Mediterranean Sea is significantly lower than over other areas (Gat and Carmi, 1970). This causes the precipitation originating from the Mediterranean Sea to be isotopically heavier than precipitation originating from the Pacific or

Atlantic Oceans.

Because the fractionation of deuterium and oxygen-18 is temperature dependent, their concentration in a water sample can lend valuable information regarding the environmental conditions at the time of condensation. Deuterium and oxygen-18 concentrations of ground water are indicative of the altitude, latitude, origin and seasonality of the recharge. Other applications using the fractionation of hydrogen and oxygen in the hydrosphere are discussed by Faure (1977, p.323).

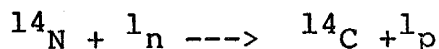
Sampling Techniques: Water samples for stable isotope analyses were taken at all eighteen field sites (Figure 2). The only sampling precaution necessary for deuterium and oxygen-18 analyses is the storing of samples in leak-tight bottles in order to prevent evaporation. Therefore, samples were collected in 250 ml glass bottles with poly-V caps and sealed with paraffin wax. Due to the ease of sampling, duplicate samples were collected.

All samples were analyzed using standard mass spectrometric techniques at the Isotope Geochemistry Laboratory, University of Arizona.

Carbon-14

Theory: The use of carbon-14 to date ground water was first suggested by Munnich (1957) and has since become an established and widely used means of determining the elapsed time between infiltration and sampling. The method consists of measuring the radiocarbon content of the dissolved carbonate in water. Due to its relatively long half-life (5730 years), carbon-14 dating is considered applicable to ages ranging from 5 to 40,000 years (Mook, 1980; van der Merwe, 1982).

Carbon-14 is produced in the upper atmosphere by several nuclear reactions. The most important is the reaction of cosmic ray thermal neutrons with nitrogen-14,



(Libby, 1965). The carbon-14 is rapidly oxidized to CO_2 and is incorporated into the atmospheric reservoir of CO_2 where ^{14}C concentrations are maintained at a relatively constant level. This equilibrium is due to the balance between (1) a continuous production of CO_2 , and (2) its continuous decay. The natural activity of carbon-14 in the atmosphere is represented by the symbol A_0 and is equal to 13.56 ± 0.07 disintegrations per minute per gram of carbon (dpm/gC).

Water, because it reacts with atmospheric CO₂, will also have a constant concentration level of carbon-14 as long as it is in equilibrium with the atmospheric reservoir. Upon infiltrating and moving beneath the water table, the water is no longer in contact with the atmosphere and the continuous supply of radiocarbon is cut off. Equilibrium between the atmosphere and the ground water no longer exists and the carbon-14 activity of the water begins to decrease due to radioactive decay. The activity at sampling is then a function of the time since entering the aquifer. In simple cases, the carbon-14 age can be calculated from the equation,

$$t = \frac{1}{\lambda} * \ln \frac{A_0}{A}$$

where λ is the decay constant and is equal to $\ln 2$ divided by the carbon-14 half life, A_0 is the initial activity of radiocarbon, and A is the measured activity.

An elementary approach to the carbon-14 method of dating ground water would rely on two assumptions. First, it would be assumed that over the past 70,000 years the natural activity of the atmosphere, and thus the hydrosphere, has not changed. Secondly, it would be assumed that there are no sources or sinks for radiocarbon once the water leaves the unsaturated zone.

The difficulties of radiocarbon dating arise in that these two assumptions are not necessarily always valid. There have been detailed studies that indicate that the natural initial activity of carbon-14 in the atmosphere has systematically varied in the past (Faure, 1977). In addition, there are chemical and isotopic reactions that occur between the water and soil or aquifer that can have significant effects on the carbon-14 activity of the water. However, these secular variations and reactions can be accounted for; thus eliminating many of the uncertainties of the dating method.

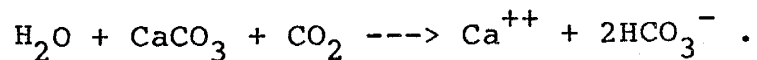
Over the past 30,000 to 40,000 years there has been a long-term natural variation in the carbon-14 activity of the atmosphere (Faure, 1977). This is due, in large part, to a change in the Earth's magnetic field. Recall that neutrons produce carbon-14 from nitrogen-14. The neutron flux is dependent on the intensity of the cosmic ray proton flux which is modulated by changes in the intensity of the Earth's magnetic field (Faure, 1977). In addition, the activity of the sun exerts some influence on the neutron flux, since many of the cosmic-ray protons are emitted by the sun. Therefore, it seems that the atmospheric activity of carbon-14 has naturally varied in the long-term past due to changes in (1) the intensity of the Earth's magnetic field, and (2) possibly the activity of the sun.

Man has influenced the atmospheric carbon-14 concentration in the past century in two ways. These fluctuations are referred to as the "Suess effect" and the "bomb effect". The Suess effect recognizes the decline in atmospheric carbon-14 with the onset of industrialization in the 1920's. Suess (1955) found that the activity of 20th-century wood is nearly 2% lower than that of 19th-century wood. He attributed this to the introduction of "dead" CO_2 into the atmosphere through the combustion of fossil fuels. According to Mook (1980), this effect can be treated as a simple linear dilution and can be corrected for just by knowing the fraction of fossil fuel derived CO_2 in the atmosphere. More importantly, the testing of nuclear bombs introduced large quantities of artificially produced carbon-14 from 1953 to 1962. This addition has temporarily increased the radiocarbon of the atmosphere twofold above normal. A gradual decrease towards normal concentrations is being observed due to exchange with the ocean (Mook, 1980).

The carbon-14 dating method assumes that the initial radiocarbon activity of the material in question was 100% of modern CO_2 activity. This assumption is, for the most part, valid when dating plant and animal remains. However, the situation is much more complicated when the material in question is water in a confined aquifer.

There are two primary types of dissolved carbon in ground water: radiocarbon from the soil zone and "dead" carbon from the aquifer matrix or carbonate cement. There are several processes which occur in each of these environments which can modify the initial carbon-14 activity. Mook (1980) discussed at length all of the possible processes, and much of the following text is taken from his work. Only those reactions which are applicable to the situation under investigation will be discussed. The first three processes occur in the unsaturated zone while the final four are reactions that occur below the phreatic surface.

Plants produce CO_2 in the soil zone due to root respiration. The CO_2 is capable of dissolving soil carbonate through the following reaction:

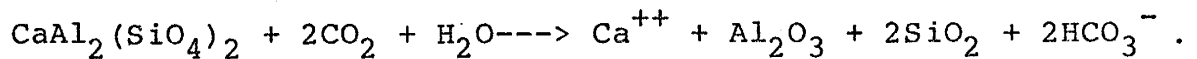


Half of the resulting bicarbonate originated from the soil carbonate (0 pmc) and the other half from the soil air (100 pmc). Consequently, the initial carbon-14 activity of the dissolved bicarbonate is expected to be 50 pmc.

Atmospheric CO_2 dissolved in precipitation can have the same effect. But due to the minor amounts of CO_2 dissolved in rain water as compared with soil air, this effect is

usually considered negligible. However, Mook (1980) cautions that in areas of very little or no vegetation, the contribution of atmospheric CO₂ may be significant.

Another reaction which affects the initial activity of ground water by adding modern carbon, is the weathering of silicate minerals (Vogel and Ehhalt, 1963). In this case, soil CO₂ contributes to erosion through the following reaction:



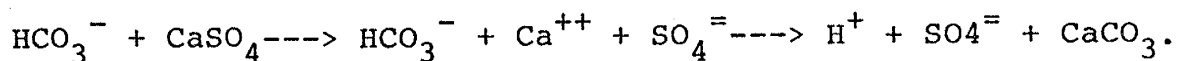
All of the carbon in the dissolved bicarbonate is from soil CO₂ and, therefore, would have a carbon-14 content of 100 pmc. This process is thought to occur at very slow rates; thus contributing only insignificant amounts of dissolved carbonate to ground water.

The initial ¹⁴C activity and carbonate concentration of ground water is determined in the vadose zone. But changes can still occur even when it is no longer in contact with the atmosphere and is in equilibrium with the aquifer. For instance, an isotopic exchange process between the ground water and the carbonate grains in the aquifer can result in a depletion of carbon-14 in the ground water. The continual decay of carbon-14 inside the carbonate grains causes a solid state diffusion of carbonate ions through the calcite

crystals (Mook, 1980). In effect, the calcite acts as a sink for dissolved carbon-14. Laboratory experiments have shown that the degree to which the carbon-14 age of the ground water is affected by this exchange process depends on (1) grain size, (2) carbonate content of aquifer relative to the dissolved carbonate in the ground water, and (3) the pH of the water (Munnich et al., 1967; Thilo and Munnich, 1970). This process probably occurs at a very small scale and is thought to be of minor significance (Mook, 1980).

If, due to Ca^{++} and Na^+ ion exchange, the ground water becomes undersaturated with respect to calcite, dissolution of CaCO_3 would result. The dissolved carbon-14 would thus be diluted by nonradiogenic carbonate. On the other hand, if the ground water becomes supersaturated with respect to calcite, due to $\text{Na}^+ - \text{Ca}^{++}$ ion exchange, CaCO_3 would precipitate out of solution. However, this reaction would not affect the radiocarbon activity of the water.

Another possible complication within the aquifer is incongruent dissolution. Take, for example, the following reactions:



The problem arises from the need to correct for both isotopic fractionation and radiogenic carbon losses with

each repeated sequence of precipitation and dissolution. With the above reaction (calcite - gypsum) the carbon-14 activity is little affected. However, this process becomes a serious complication in the case of calcite - dolomite incongruent dissolution. Evans et al. (1979) presented a simplified formula for the correction of carbon-14 activity measurements when the ground water has been affected by incongruent dissolution.

One final consideration in radiocarbon dating is the fractionation that occurs with the transfer of carbon from one reservoir to another. Corrections must be made in order to obtain an accurate initial carbon-14 concentration. Carbon-14 activity is affected by both radioactive decay and fractionation, but the two effects are indistinguishable. It is for this reason that carbon-13 (nonradioactive) is used to determine the degree to which carbon-14 is fractionated. Since carbon-14 is one neutron heavier than carbon-13 it will be fractionated twice as much (Bigeleisen, 1952; Craig, 1954). Knowing this, the fractionation of carbon-14 can be corrected for through the use of carbon-13. Additionally, of course, measuring the carbon-13 concentration of ground water provides a means to correct for the addition of "dead" carbon due to limestone dissolution.

Sampling Techniques: Water samples for carbon-14 analyses were taken at all sample locations except SJB-18-OA and SJB-19-OA. It was noted in the field that the apparent carbon-14 date for SJB-17-OA would represent only a minimum age due to the possibility of re-equilibration with the atmosphere.

A fairly complex procedure is required for carbon-14 field sampling. The procedure followed is that outlined by the Australian Atomic Energy Commission and is included in Appendix II. Dissolved carbon was precipitated out of a water sample by adding saturated BaCl_2 to water with a pH greater than 8. This pH was maintained by the addition of carbonate-free NaOH. A carbon-free flocculant was added to hasten the coagulation of BaCO_3 . The slurries were tightly sealed in 1 liter polyethylene containers. In addition, temperature measurements and alkalinity titrations were performed in the field.

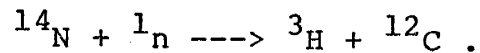
It is necessary to take several precautions when sampling water for carbon-14 analysis. The primary consideration was that the sample not be contaminated with modern carbon. This requires that (1) the well or spring is algae-free, (2) the water sample is exposed to the atmosphere as little as possible, (3) a steady flow of water into the precipitation carboy is maintained, with as few air

bubbles as possible, and (4) the water sample is representative of the aquifer (i.e., remove bore-hole water before taking sample).

All carbon-14 analyses were performed at the Isotope Geochemistry Laboratory of the University of Arizona under the direction of Dr. Austin Long. Samples 1 through 12 and 17 were analyzed by gas proportional counting while samples 13, 14 and 15 were analyzed by tandem-accelerator mass spectrometry.

Tritium

Theory: Tritium, the radioactive isotope of hydrogen, has a half-life of 12.35 years (Fontes, 1980). It is naturally produced in the upper atmosphere by secondary neutrons interacting with nitrogen:



The tritium atom is very reactive and is quickly incorporated into the hydrologic cycle as HTO molecules.

Through the natural production of tritium and its radioactive decay, a steady state concentration in the atmosphere was maintained before human activities influenced tritium levels. Concentrations are measured in tritium units (TU), where one TU equals 10^{18} hydrogen atoms for

every one tritium atom. The natural concentration ranges between 4 and 25 TU, with New Mexico having concentrations between 10 and 15 TU. The concentration of tritium in precipitation varies with latitude, altitude, and season. Concentrations increase away from the equator, and the maximum activity in rainfall is during the spring. Gat (1980) discussed the stratospheric-tropospheric relationship which causes these dependencies.

The atmospheric testing of nuclear bombs between 1953 and 1962 introduced copious amounts of artificial tritium to the atmosphere. Northern hemisphere levels peaked at approximately 2000 TU in 1963; however, in the southern hemisphere tritium concentrations peaked in 1966 at 100 TU. The discrepancy in the two maximum values is attributed to the larger percentage of testing having been conducted in the northern hemisphere. Since 1963, tritium levels in precipitation have been approaching natural levels at an exponential rate. The present level in New Mexico precipitation is between 40 and 50 TU.

Tritiated water enters an aquifer in its recharge zone. A water sample with measureable tritium levels would not have been in the aquifer for very long, due to its short half-life, and thus would indicate active recharge areas. A simplified age interpretation of tritium concentrations was

outlined by the IAEA (1973):

<u>TU</u>	<u>AGE</u>
<3	> 30 years
3-20	30-20 years
>20	< 20 years

Sampling Techniques: Samples for tritium analyses were taken at sites SJB-01-OA through SJB-16-OA (Figure 2). One liter polyethylene bottles were used for containers. No stringent sampling precautions are necessary for tritium, but contact with modern water or water vapor must be avoided.

All samples were analyzed at New Mexico Institute of Mining and Technology by Dr. Gerardo Gross using electrolytic enrichment and proportional counting methods.

Noble Gases

Theory: The noble gases, neon, argon, krypton, and xenon are produced naturally in the atmosphere. They are inert and stable. Under equilibrium conditions their solubility will depend on the ambient air temperature. Aquifer-recharge water normally contains dissolved noble gases in equilibrium with the atmosphere at the prevailing

vadose zone temperature, and due to the chemical inertness of the gases their concentrations will not change during transit. Therefore, measurement of noble gas concentrations upon discharge can give information concerning climatic conditions at the time of recharge.

The use of noble gases to determine recharge temperatures was first investigated by Sugisaki (1961). Using the principles of noble gas solubility, he was able to determine flow velocities in a shallow aquifer in Japan. Later studies by Mazor and Wasserburg (1965) and Mazor and Fournier (1972) used noble gas concentrations in ground water to determine the origin of geothermal water. Recently, Phillips (1981) presented a comprehensive look at the use of noble gases in ground water as paleoclimatic indicators.

Sampling Techniques: Samples for noble gas analysis were taken at two locations, SJB-04-OA and SJB-11-OA (Figure 2). The small number of samples obtained was due to the lack of appropriate sampling locations. Samples were collected and stored in lengths of copper tubing sealed at each end with pinch-off clamps. Triplicate samples were taken at each site.

Several precautions are necessary when sampling for noble gas analysis. First, the water reservoir from which the sample is to be taken can not have had the chance to re-equilibrate with the atmosphere. This eliminates springs without a specific discharge point, wells with pressurized tanks, and wells with leaks in the pipes. In addition, it is of extreme importance to eliminate any entrapped air in the sample container. According to Phillips (1981), as little as .04 percent air could cause a 1 °C error in calculated temperatures.

Noble gas analyses will be performed by Dr. Stanley Davis, Department of Hydrology and Water Resources, University of Arizona using gas chromatograph - mass spectrometric techniques.

HYDRAULICS OF THE OJO ALAMO SANDSTONE

Existing transmissivity data for the Ojo Alamo Sandstone are scarce. Most measurements (Lyford, 1979; Stone, 1979c) indicate transmissivity values of $10 \text{ m}^2/\text{day}$ ($108 \text{ ft}^2/\text{day}$) or less. An aquifer test performed in 1957 by Bushman and Foster using a well in Cuba gave transmissivities between 9 and $12 \text{ m}^2/\text{day}$ (100 and $130 \text{ ft}^2/\text{day}$) (Anderholm, 1979). Brimhall (1973) reported transmissivity values ranging from 5 to $15 \text{ m}^2/\text{day}$ (57 to $165 \text{ ft}^2/\text{day}$) from six pump tests conducted between Cuba and Farmington. Anderholm (1979) conducted a pumping test using a well southwest of Cuba and found the transmissivity to be $8.5 \text{ m}^2/\text{day}$ ($91 \text{ ft}^2/\text{day}$). Based on this information, it is the opinion of the authors that a transmissivity of $10 \text{ m}^2/\text{day}$ ($108 \text{ ft}^2/\text{day}$) is a representative value for the Ojo Alamo aquifer.

Figures 5 and 6 are water level elevation maps for the Ojo Alamo Sandstone and the Nacimiento Formation. Depth to water data from Stone et al. (1983) were used to construct the maps for the Ojo Alamo Sandstone and Nacimiento Formation. The equipotential lines on both maps suggest that ground-water flow is generally to the north, towards the San Juan River (Figure 7). It should be noted that the equipotential lines in most of Rio Arriba County are hypothetical due to the lack of measurement points. Berry

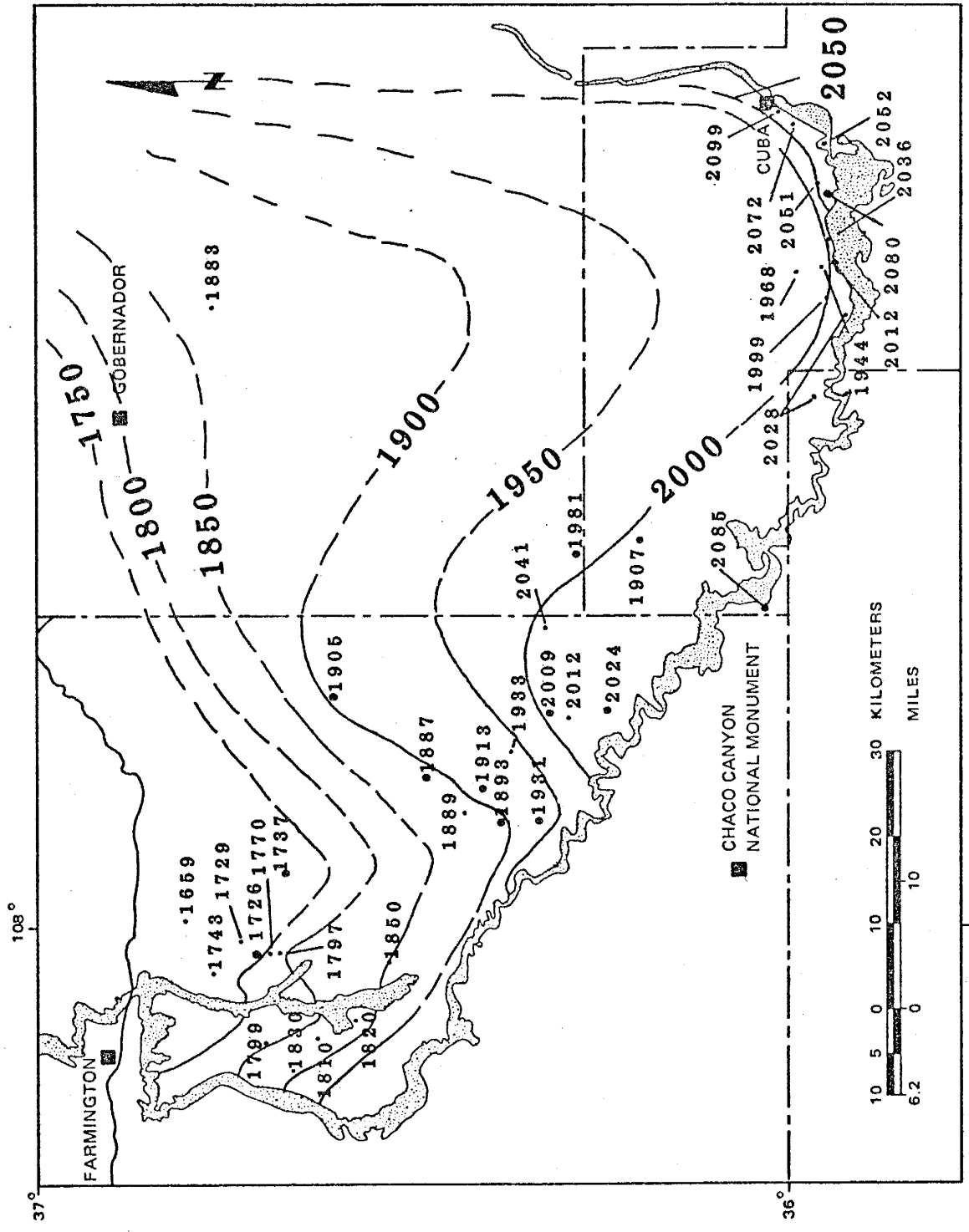


Figure 5. Potentiometric surface map for the Ojo Alamo Sandstone (elevation in meters).

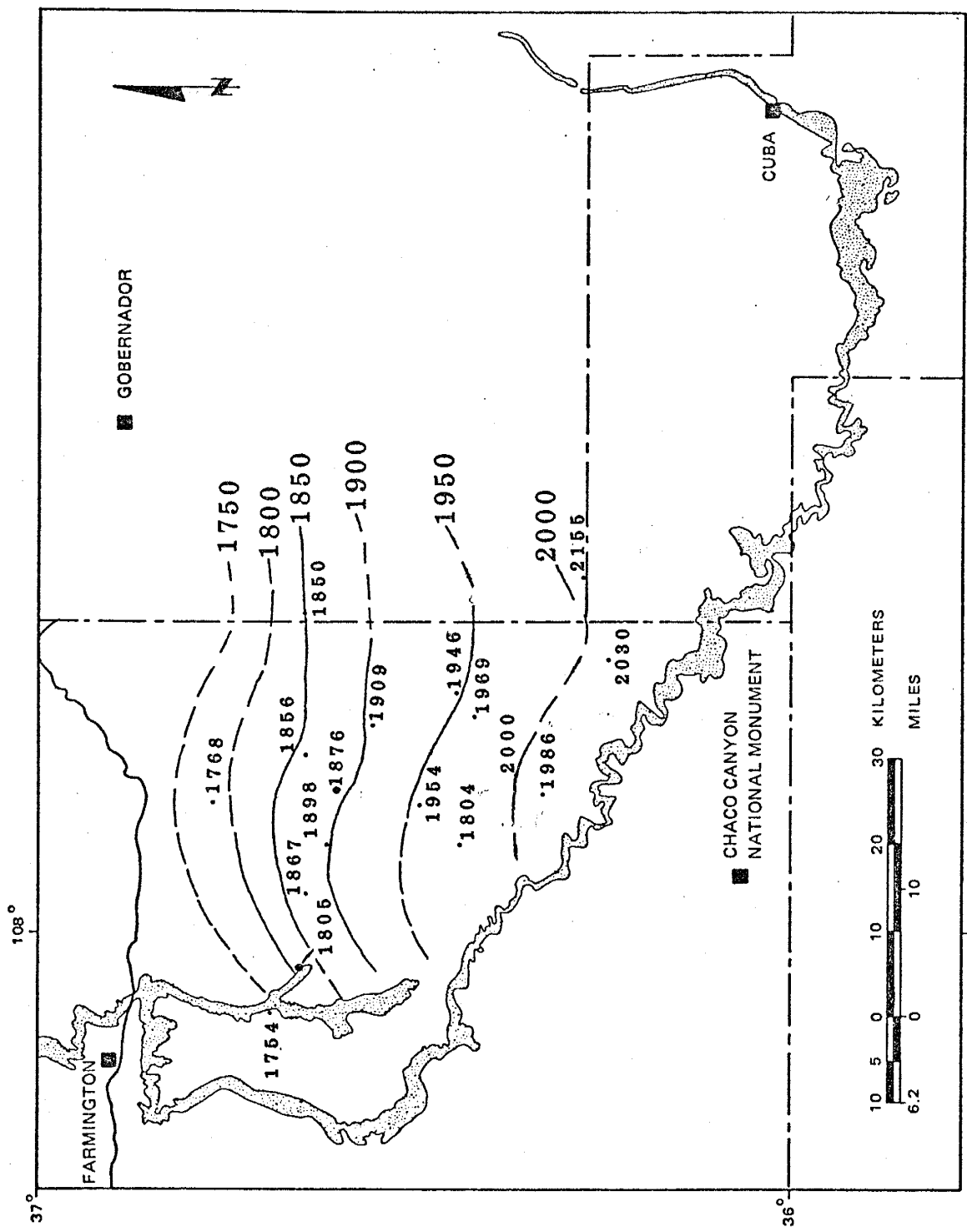


Figure 6. Potentiometric surface map for the Nacimiento Formation (elevation in meters).

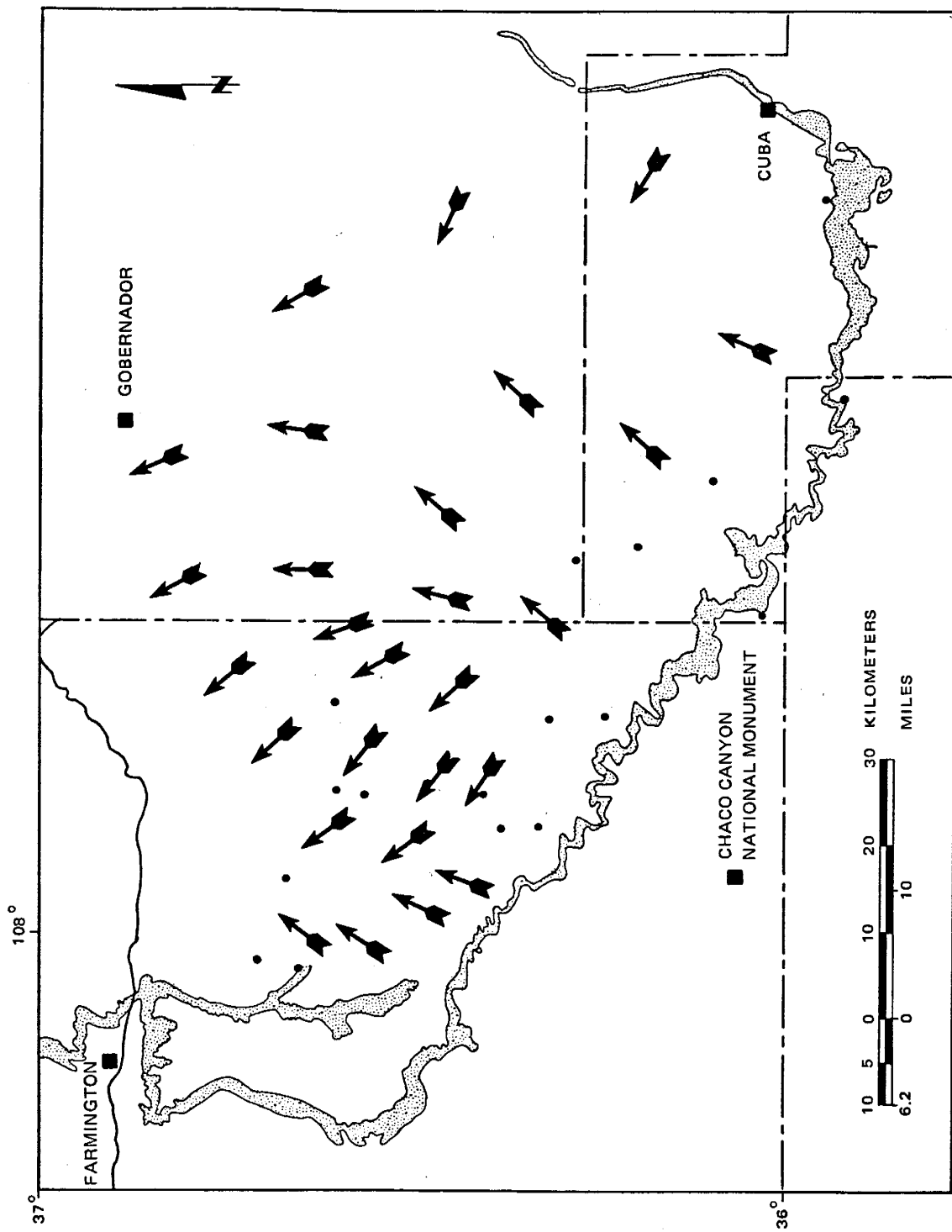


Figure 7. General flow directions for ground water in the Ojo Alamo Sandstone.

(1959) presented a potentiometric surface map for the Pictured Cliffs Sandstone, the aquifer immediately below the Fruitland Formation.

Vertical head gradients between the Ojo Alamo Sandstone and the Nacimiento Formation, and the Ojo Alamo and the Pictured Cliffs Sandstones were calculated by overlaying the two potentiometric surface maps and taking the difference in head where two contours cross. Figures 8 and 9 are maps showing the distribution of vertical head for the study area. A positive value indicates an area of possible downward leakage and a negative value suggests upward leakage. Figure 8 shows that over most of the area the head in the Nacimiento Formation is higher than the head in the Ojo Alamo Sandstone; therefore, downward leakage should be considered. Likewise, Figure 9 shows a positive head differential between the Ojo Alamo and the Pictured Cliffs Sandstones over most of the study area. Thus, water may be leaking out of the Ojo Alamo Sandstone and into the Cretaceous strata.

In order to determine whether leakage into or out of the Ojo Alamo Sandstone is of significance, the horizontal flux (Q_h) was calculated and compared with the vertical fluxes (Q_v) for the adjacent units. Assigning an average thickness of 53 m and a transmissivity of $10 \text{ m}^2/\text{day}$ to the Ojo Alamo Sandstone, the hydraulic conductivity, K , was determined to be $.19 \text{ m/day}$. The regional head gradient,

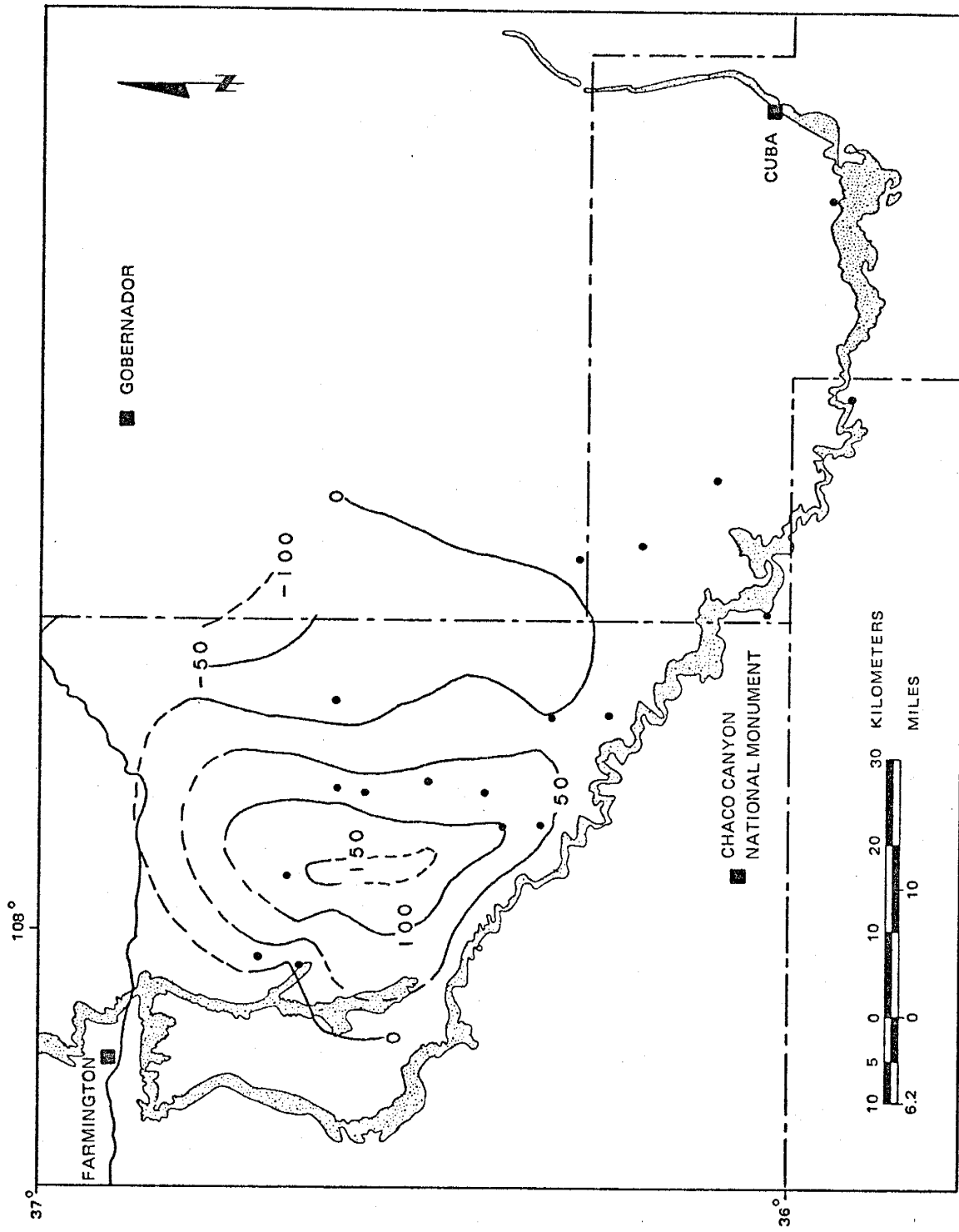


Figure 8. Vertical head gradient between the Nacimiento Formation and the Ojo Alamo Sandstone (positive value indicates a downward gradient).

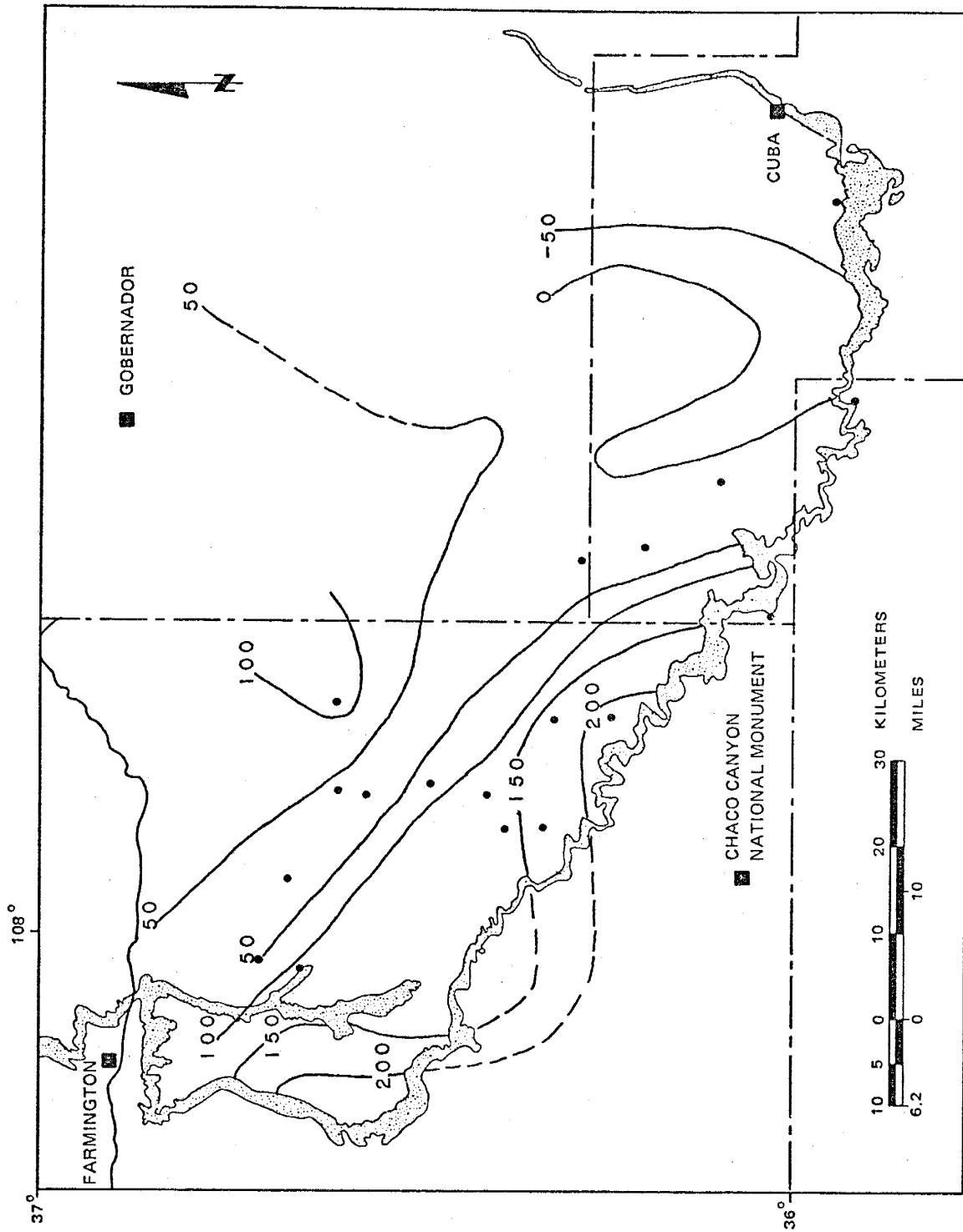


Figure 9. Vertical head gradient between the Ojo Alamo and the Pictured Cliffs Sandstones (positive value indicates a downward gradient).

dH/dl , along a 1 km wide flow path was estimated to be 250 m of head drop over 30 km (Figure 5). Using Darcy's Law, $Q = K \times A \times (dH/dl)$, the horizontal flux through a 1 km by 53 m flow tube was calculated to be $100 \text{ m}^3/\text{day}$.

Estimating the vertical fluxes from the adjacent units is slightly more complicated. The hydraulic conductivity for shales ranges from 10^{-13} to 10^{-10} m/sec (Freeze and Cherry, 1979, p.29). An intermediate value of 10^{-12} m/sec (8.6×10^{-8} m/day) was assigned to the Nacimiento Formation and the Kirtland Shale. Minimum thicknesses were used so as to be as liberal as is justified in determining the vertical fluxes. A general flow path was traced using the potentiometric surface maps in order to estimate the average vertical head differential. The vertical flux for a 1 km^2 interface was then calculated using Darcy's Law. However, to determine the total volume of water entering or leaving the Ojo Alamo Sandstone from adjacent units (along the same flow path used for the horizontal flux of the Ojo Alamo) Q_v/km^2 must be multiplied by the length of the flow path (in this case, 30 km). The following table summarizes the values used in estimating Q_h and Q_v .

	TKoa	Tn	Kkf
K (m/day)	.19	8.6×10^{-8}	8.6×10^{-8}
dH_v (m)		100	-100
dH_h (m)	250		
dl_v (m)		127	152
dl_h (m)	30,000		
area (m ²)	53,000	1×10^6	1×10^6
Q_v/km^2 (m ³ /day/km ²)		.068	-.057
Q_h (m ³ /day)	100		
Q_v (m ³ /day)		2.04	-1.71

The Ojo Alamo Sandstone receives from the Nacimiento Formation approximately 2 m³ of water per day along a 30 km long by 1 km wide flow path. This amounts to about 2% of the 100 m³/day horizontal flow in the Ojo Alamo along the same flow path. On the other hand, the Ojo Alamo Sandstone loses about 1.7 m³ of water per day, or a little less than 2% of its volume, to downward leakage. It appears then, that leakage into or out of the Ojo Alamo Sandstone will not seriously effect ground-water dates. However, these calculations are based on estimates. The application of a 3-D model to determine leakage fluxes would eliminate much of the estimating and thus give more reliable results. But the value chosen for the hydraulic conductivity, which may naturally vary by four orders of magnitude, is more important. Although the hydraulic conductivities assigned to the Nacimiento Formation and Kirtland Shale are well within reason, a verified value would substantiate

conclusions regarding leakage.

The porosity, n , of the Ojo Alamo Sandstone was determined in the laboratory using the equation:

$$n = 1 - (\rho_b / 2.65) \times 100$$

where ρ_b , the bulk density, is equal to the dry weight of the rock sample divided by the total volume of the sample. The sample was collected from an outcrop near Ojo Socorro. Three weighings resulted in an average dry weight of 468.40 grams. The rock sample was then coated with a thin layer of paraffin wax and submerged in a known volume of water. 220 milliliters of water were displaced, resulting in a porosity of 20%.

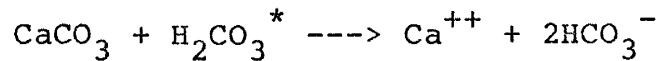
MODELS

Vogel's Approach

Vogel (1967, 1970) developed an empirical method for assigning the initial carbon-14 activity. Based on radiocarbon measurements of 100 modern ground-water samples in northwest Europe, Vogel proposed a value of 85 ± 5 pmc for the initial radiocarbon activity of ground water. His approach did not consider isotopic exchange beneath the phreatic surface and may not be applicable to arid or semi-arid climates.

Tamers' Model

Tamers' (1967, 1975) model accounts for limestone dilution through the use of dissolved carbonate species concentrations. Considering the reaction for the dissolution of limestone,



it is evident that only one half of the bicarbonate carbon is of atmospheric origin. Therefore, in the normal pH range of ground waters, the dilution of radiocarbon due to dissolution of limestone can be expressed as:

$$A_o = \frac{m\text{CO}_2 + 0.5m\text{HCO}_3^-}{m\text{CO}_2 + m\text{HCO}_3^-} A_g$$

where m represents the molality and A_g is the carbon-14 activity of the soil gas, normally assumed to be 100 pmc. This approach assumes that the activity of the dissolving

mineral carbonate is zero. However, such is not always the case. Therefore, the activity of the soil carbon should be taken into consideration by using the equation:

$$A_o = \frac{(mCO_2 + 0.5mHCO_3^-)A_g + (0.5mHCO_3^-) A_c}{mCO_2 + mHCO_3^-}$$

where A_c is the activity of the mineral carbonate. This equation can be expressed in another form where the pH and activity of the soil carbonate are the only variables:

$$A_o = (100\text{pmc} - A_c) \frac{2 * 10^{-\text{pH}} + 10^{-6.3}}{2(10^{-\text{pH}} + 10^{-6.3})} + A_c$$

As previously mentioned, these equations are applicable to ground waters with pH's ranging from 5 to 8. Due to the basic nature of the water in the Ojo Alamo Sandstone, it was necessary to modify the equations in order to account for $CO_3^{=}$ concentrations. The following equation assumes that all dissolved carbonate had a mineral origin, and thus zero activity, and was the form of Tamers' equation used to determine the initial activity of the ground-water samples for the current project:

$$A_o = (100\text{pmc} - A_c) \frac{2 * 10^{-\text{pH}} + 10^{-6.3}}{2(10^{-\text{pH}} + 10^{-6.3} + 10^{-16.6+\text{pH}})} + A_c$$

Pearson's Model

Ingerson and Pearson (1964) suggested a method which accounts for the dilution of biogenic carbon by mineral carbonate by using measurements of the $\delta^{13}C$ of the

ground-water sample. Carbonates of marine origin typically have a $\delta^{13}\text{C}$ of 0 ‰ relative to the PDB standard. Fresh water limestones and soil carbonates are usually depleted in carbon-13 with respect to the standard, and thus have slightly negative $\delta^{13}\text{C}$ values. On the other hand, the $\delta^{13}\text{C}$ of soil gas can vary drastically. The controlling factor is the type of photosynthetic pathway followed by the plants in the recharge area. There are basically two types of photosynthetic cycles: the Calvin cycle (C3) and the Hatch-Slack cycle (C4). Soil CO_2 produced by C3 plants will have an average $\delta^{13}\text{C}$ of -26.5 ‰, but may vary from -20 ‰ to -35 ‰ depending on the environmental conditions. C4 plants typically produce soil gas with $\delta^{13}\text{C}$'s averaging close to -12 ‰ but ranging from -9 ‰ to -16 ‰. van der Merwe (1982) discussed these two photosynthetic pathways and the resulting carbon fractionation.

By taking into account the fact that mineral carbonate has a distinctly different $\delta^{13}\text{C}$ than biogenic soil gas, it is possible to determine the initial carbon-14 activity of a water sample using an isotope mixing model:

$$A_o = \frac{\delta_o - \delta_c}{\delta_g - \delta_c} (A_g - A_c) + A_c$$

where δ_o , δ_g and δ_c are the carbon-13 contents of the water, soil gas and mineral carbonate, respectively and A_g and A_c are the radiocarbon activities of the soil gas and mineral carbonate. Accounting for isotopic fractionation, the

previous equation becomes:

$$A_o = [(A_g - .2\epsilon_2) - (A_c - .2\epsilon_9)] \frac{\delta_o - (\delta_c + \epsilon_9)}{(\delta_g - \epsilon_2) - (\delta_c + \epsilon_9)} + (A_c - .2\epsilon_9)$$

where ϵ_2 and ϵ_9 are the fractionation factors for CO_2 to bicarbonate and bicarbonate to CaCO_3 , respectively.

Mook's Approach

Mook (1972, 1976) presents a model that not only takes into account dissolution of soil carbonate but also considers isotopic exchange in the unsaturated zone, between dissolved bicarbonate and soil gas. Using a mass balance, Mook derives the following equation for the initial carbon-14 activity of a ground-water sample:

$$A_o = \frac{a}{\Sigma} A_{ao} + 0.5 \left[1 - \frac{a}{\Sigma} \right] (A_{ao} + A_{lo}) + [A_{go} (1 - 2 \times 10^{-3} \epsilon_g) - 0.5 (A_{ao} + A_{lo})] \cdot \frac{\delta_\Sigma - (a/\Sigma) \delta_{ao} - 0.5 [1 - (a/\Sigma)] (\delta_{ao} + \delta_{lo})}{\delta_{go} - \epsilon_g (1 + 10^{-3} \delta_{go}) - 0.5 (\delta_{ao} + \delta_{lo})}$$

where

A = carbon-14 activity, pmc;

δ = carbon-13 concentration, per mille versus PDB;

Σ = molal concentration of total dissolved carbon;

a = molal concentration of aqueous CO_2 ;

ϵ_g = isotopic enrichment factor between gaseous CO_2 and HCO_3^- , in per mille

l, g, o = limestone, gaseous CO_2 , and initial contents, respectively.

This equation is based on three processes: (1) soil carbonate reacting with dissolved CO_2 in the unsaturated zone, (2) isotopic exchange between bicarbonate and soil gas in the unsaturated zone, and (3) an additional amount of CO_2 added to chemically stabilize the solution. Dissolution or precipitation of mineral carbonate within the aquifer is not taken into consideration nor is isotopic exchange between the solution and the soil carbonate.

Mook's equation is essentially the same as Tamers' equation but with an added correction term, K , accounting for isotopic exchange. The first two terms in Mook's equation refer to the dissolution process while the third term represents isotopic exchange. Therefore, the equations from the two models are equivalent when isotopic exchange is negligible.

Fontes' Model

Like Mook's model, Fontes and Garnier (1979) used a chemical mass balance equation along with a correction term for isotopic exchange to determine the initial activity of carbon-14. However, this model considers exchange between (1) mineral carbonate and soil CO_2 and (2) dissolved carbonate and mineral carbonate.

Limestone (or soil carbonate) dilution is best determined using the field-measured alkalinity. From an alkalinity titration curve, the molal concentrations of

carbonate, bicarbonate and carbonic acid can be calculated and then used to figure the molal concentrations of inorganic carbon (mC_M) using:

$$mC_M = \frac{2mCO_3^{=} + mHCO_3^{-}}{2}$$

In addition, the molal concentration of total dissolved carbon (mC_T) is determined using:

$$mC_T = mCO_3^{=} + mHCO_3^{-} + mH_2CO_3^*$$

Fontes' model accounts for isotopic exchange within the carbonate reaction series by considering a simple two term exchange-mixing process between the two end members, gaseous CO_2 and $CaCO_3$.

If the concentration of soil CO_2 is the controlling factor for isotopic exchange, the following mass balance equation represents the process:

$$\delta_T C_T = (C_M - q) \delta_M + (C_T - C_M) \delta_g + q(\delta_g - \epsilon)$$

On the other hand, if exchange is controlled by the $CaCO_3$ concentration it is accounted for by:

$$\delta_T C_T = C_M \delta_M + (C_T - C_M - q') \delta_g + q'(\delta_M + \epsilon)$$

where

q = molal concentration of 'solid' carbonate at equilibrium with an excess of soil CO_2 ;

q' = molal concentration of 'active' carbon at equilibrium with solid carbonate;

ϵ = isotopic enrichment factor between gaseous CO_2 and solid carbonate, in per mille;

T, M, g = total, solid, and gaseous carbon, respectively.

Solving the equations for q and q', it is seen that the equations are opposite, that is, $q = -q'$. Consequently, the single equation

$$q = -q' = \frac{\delta_T C_T - C_M \delta_M - \delta_g (C_T - C_M)}{\delta_g - \epsilon - \delta_M}$$

accounts for both exchange reactions. If the calculated q is greater than zero then exchange is controlled by soil CO_2 and if q is less than zero exchange is controlled by mineral carbonate.

An analogous mass balance equation for ^{14}C can be written as follows:

$$A_o C_T = C_M A_M + (C_T - C_M) A_g + q(A_g - 0.2\epsilon - A_M)$$

Solving for A_o and substituting in q results in the following expression for the initial activity of the total dissolved carbon:

$$A_o = \left(1 - \frac{C_M}{C_T}\right) A_g + \frac{C_M}{C_T} A_M + (A_g - 0.2\epsilon - A_M) \cdot \frac{\delta_T - (C_M/C_T)\delta_M - [1 - (C_M/C_T)]\delta_g}{\delta_g - \epsilon - \delta_M}$$

The first two terms are equivalent to the equation for Tamers' model while the third is the correction for isotopic exchange. When isotopic exchange is insignificant, Fontes' equation tends towards Tamers' expression.

RESULTS

Stable Isotopes

Stable isotope analyses were performed on all eighteen water samples. The results of the analyses are presented in Table 2 and are plotted at the respective sample sites in Figure 10. The general trend is a decrease in oxygen-18 and deuterium content corresponding to an increase in travel distance. The three spring samples near the outcrop have the heaviest isotopic composition while the wells furthest from the recharge area have water with the lightest composition. A graph of δD versus $\delta^{18}O$ highlights this trend (Figure 11). The springs plot together in the isotopically heavy corner and the most distant samples are clustered in the isotopically light corner.

Carbon-14

Laboratory analyses for carbon-14 result in values for the radiocarbon activity at the time of sampling (A) and the isotopic enrichment of carbon-13 relative to the PDB standard ($\delta^{13}C$). Table 3 presents these results for each sample.

Carbon-14 analyses were not performed on samples SJB-18-OA and SJB-19-OA. At these locations it was not possible to obtain water samples directly from the aquifer. Therefore, due to re-equilibration with the atmosphere, age

Sample #	Name	δD	$\delta^{18}O$
SJB-01-OA	Lybrook	-102	-13.2
SJB-02-OA	B of C Mission	-112	-13.3
SJB-03-OA	Pete Spring	- 81	- 9.0
SJB-04-OA	Powerline WM	- 83	-11.5
SJB-05-OA	Kimbeto WM	-113	-13.4
SJB-06-OA	Ojo Socorro	- 73	- 8.5
SJB-08-OA	Dzilth	- 93	-11.5
SJB-09-OA	Ojo Encino	- 83	- 9.1
SJB-10-OA	Johnson's TP	- 95	-12.4
SJB-11-OA	Huerfano #2	-112	-15.6
SJB-12-OA	Huerfano #1	-108	-14.5
SJB-13-OA	Nageezi CH	-103	-13.8
SJB-14-OA	Chaco Camp #9	-111	-14.1
SJB-15-OA	Hilltop	-114	-14.8
SJB-16-OA	Kah-Des-Pah	-111	-14.6
SJB-17-OA	Tsah Tah	- 90	-11.3
SJB-18-OA	Sisnathyel	-108	-13.7
SJB-19-OA	Chimney Dam	-109	-13.4

Table 2. Isotopic enrichment of D and ^{18}O in per mille relative to SMOW; analytical precision of measurements is ± 3 ‰ and ± 0.2 ‰, respectively.

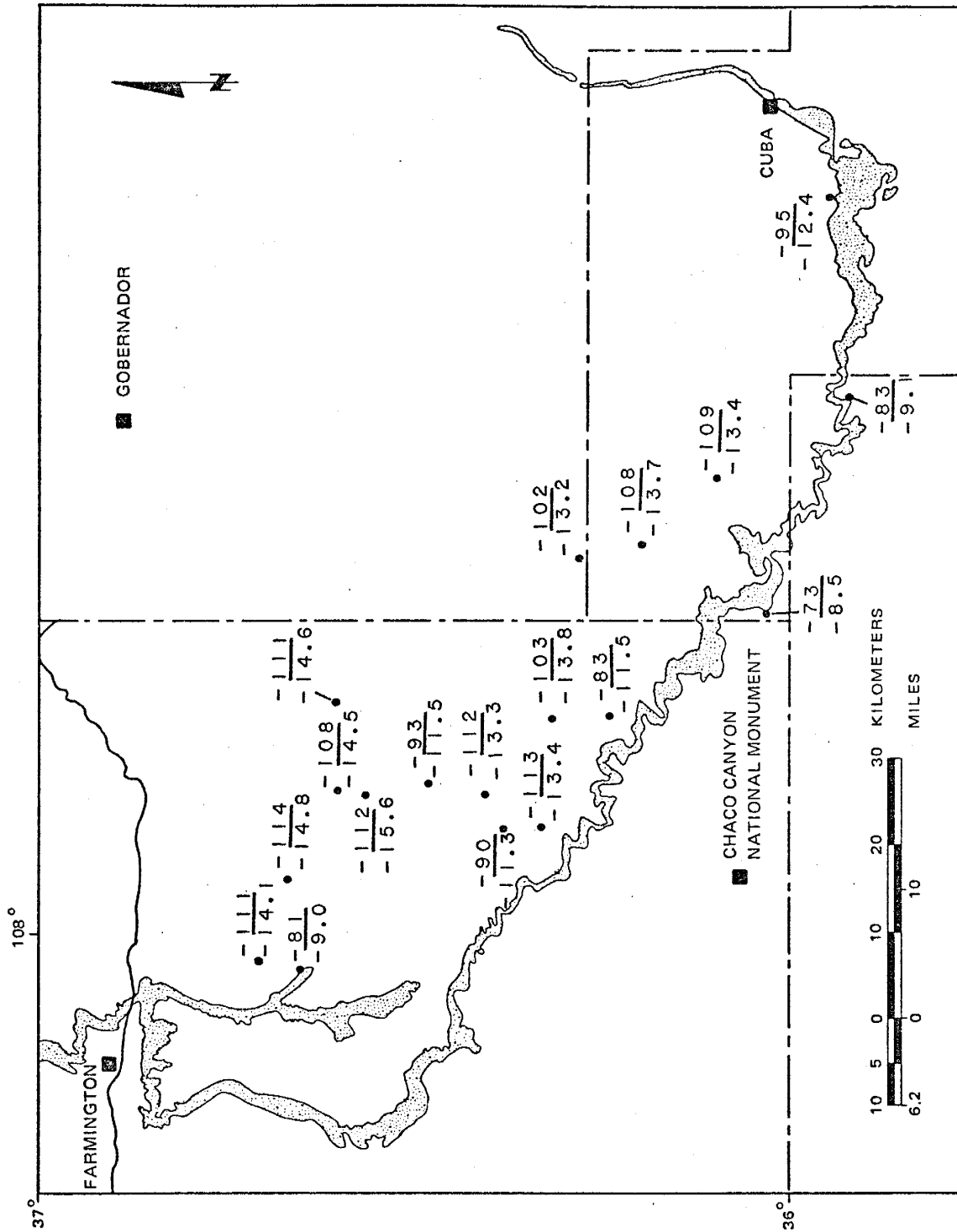
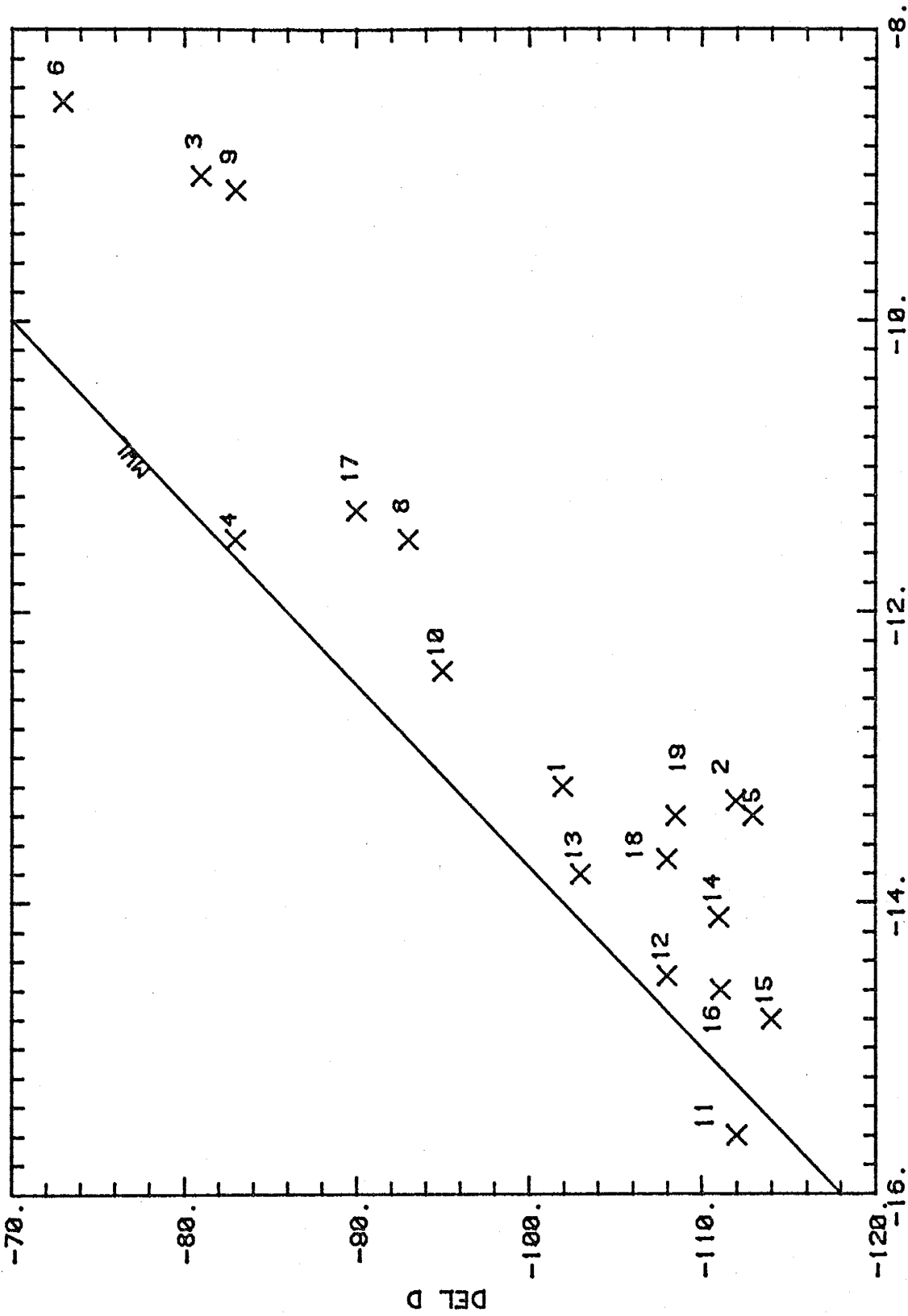


Figure 10. Map of $\delta D/\delta^{18}O$ (in per mille relative to SMOW).



DEL 18-0

Sample #	Name	A (pmc)	$\delta^{13}\text{C}$
SJB-01-OA	Lybrook	6.88 +/- 0.74	-14.5
SJB-02-OA	B of C Mission	28.66 +/- 0.85	-14.1
SJB-03-OA	Pete Spring	76.33 +/- 1.44	- 8.6
SJB-04-OA	Powerline WM	51.22 +/- 1.14	-14.0
SJB-05-OA	Kimbeto WM	5.52 +/- 0.85	-14.5
SJB-06-OA	Ojo Socorro	59.34 +/- 1.96	- 6.7
SJB-08-OA	Dzilth	8.99 +/- 0.90	-16.6
SJB-09-OA	Ojo Encino	99.94 +/- 2.19	- 8.1
SJB-10-OA	Johnson's TP	51.92 +/- 1.00	-14.3
SJB-11-OA	Huerfano #2	4.70 +/- 0.6	-15.5
SJB-12-OA	Huerfano #1	4.40 +/- 1.5	-13.8
SJB-13-OA	Nageezi CH	10.16 +/- 0.56	***
SJB-14-OA	Chaco Camp #9	13.30 +/- 0.63	***
SJB-15-OA	Hilltop	10.24 +/- 0.75	***
SJB-16-OA	Kah-Des-Pah	3.50 +/- 0.7	-15.1
SJB-17-OA	Tsah Tah	40.30 +/- 0.9	-13.1

Table 3. ^{14}C activity in percent modern carbon and ^{13}C enrichment relative to the PDB standard in per mille.

determinations from these two sites would be of little value.

$\delta^{13}\text{C}$ values for water samples from Nageezi Chapter House, Chaco Camp #9 and Hilltop Liquor Store were not determined. A problem with low CO_2 yields from the BaCO_3 precipitate was encountered during analysis, making the proportional counting method unsatisfactory for these three samples. Instead, it was necessary to use the Tandem-Accelerator Mass Spectrometer, which can analyze much smaller samples. Carbon-13 concentrations were not measured due to the possibility of fractionation resulting from incomplete precipitation.

The data from Table 3 along with chemical data (Tables 4 and 5) were used to determine the initial carbon-14 activities for each water sample. Calculated A_0 values, for each of the five models are listed in Table 6. Initial activities for the three samples without $\delta^{13}\text{C}$ values were calculated using a $\delta^{13}\text{C}$ of -15.2 ‰, which is an average from the most proximal sample sites. Nonmeasured parameters were assigned the following values: activity of the mineral carbonate = 0 pmc; activity of the soil gas = 100 pmc; $\delta^{13}\text{C}$ of the mineral carbonate = 0 ‰; $\delta^{13}\text{C}$ of the soil gas = -25 ‰. Having determined the initial activity, the age of the water was then calculated using the general law governing radioactive decay:

$$t = \frac{1}{\lambda} * \ln \frac{A_0}{A}$$

Sample #	Ca ⁺⁺	Mg ⁺⁺	Na ⁺	HCO ₃ ⁻	CO ₃ ⁼	Cl ⁻	SO ₄ ⁼	pH	EC	Temp
SJB-01-OA	1.7	0.0	250	303.78	25.20	7.5	230	9.48	930	24.8
SJB-02-OA	1.0	0.0	180	266.57	42.60	3.6	91	9.62	630	15.8
SJB-03-OA	---	---	---	297.01	0.0	---	---	7.88	1050	14.5
SJB-04-OA	1.0	.6	270	290.36	17.40	6.4	340	8.96	990	16.0
SJB-05-OA	15	4.3	450	234.48	13.68	92	660	8.51	1500	13.5
SJB-06-OA	60	3.5	21	74.48	5.28	5.1	100	8.26	385	11.0
SJB-08-OA	1.6	0.0	260	115.47	26.70	8.5	110	8.68	1000	22.0
SJB-09-OA	11	.9	43	46.91	0.0	9.2	48	7.36	260	10.0
SJB-10-OA	3.9	.02	190	330.38	40.74	3.0	160	9.26	680	14.0
SJB-11-OA	10	t	243	270.72	0.0	8	315	8.47	970	17.5
SJB-12-OA	0.0	0.0	158	323.97	68.28	6	91	9.23	780	16.0
SJB-13-OA	4.0	t	290	270.72	47.76	22	310	9.32	980	18.0
SJB-14-OA	48	8	250	220.21	0.0	14	335	8.18	1000	18.0
SJB-15-OA	21	1.3	170	240.22	0.0	4.4	300	8.33	600	15.0
SJB-16-OA	4.7	.03	200	292.19	55.92	5	154	9.27	680	15.5
SJB-17-OA	4.1	.04	240	342.70	64.86	6	---	9.11	650	--
SJB-18-OA	5.0	.04	320	369.05	72.00	11	---	9.04	820	--
SJB-19-OA	--	---	---	192.58	46.86	7.0	---	9.36	590	--

Table 4. Chemical analyses for samples (ion concentrations in mg/l; t indicates trace amount present). Carbonate, bicarbonate, pH, EC and temperature values were determined from field measurements performed by the authors. Chemical analyses for:

SJB-1,2,3,4,5,6,9,13,19-OA from Stone et al., (1983)

SJB-8,10,15,16,17,18-OA analyzed by N.M.B.M.M.R.

SJB-11,12,14-OA provided by El Paso Natural Gas Co.

Sample #	Ca ⁺⁺	Mg ⁺⁺	Na ⁺	HCO ₃ ⁻	CO ₃ ⁼	Cl ⁻	SO ₄ ⁼
SJB-01-OA	.08	0	10.87	4.98	.84	.21	4.79
SJB-02-OA	.05	0	7.83	4.37	1.42	.10	1.89
SJB-03-OA	---	---	---	4.87	0	---	---
SJB-04-OA	.05	.05	11.74	4.76	.58	.18	7.08
SJB-05-OA	.75	.35	19.57	3.84	.46	2.59	13.74
SJB-06-OA	.99	.29	.91	1.22	.18	.14	2.08
SJB-08-OA	.08	0	11.31	1.89	.89	.24	2.29
SJB-09-OA	.55	.07	1.87	.77	0	.26	1.00
SJB-10-OA	.19	.00	8.26	5.42	1.36	.08	3.34
SJB-11-OA	.50	0	10.57	4.44	0	.23	6.56
SJB-12-OA	.0	.0	6.87	5.31	2.28	.17	1.89
SJB-13-OA	.20	0	12.61	4.44	1.59	.62	6.45
SJB-14-OA	.40	.66	10.87	3.61	0	.39	6.97
SJB-15-OA	.05	.11	7.39	3.94	0	.12	6.25
SJB-16-OA	.23	.00	8.70	4.79	1.86	.14	3.21
SJB-17-OA	.20	.00	10.44	5.62	2.16	.17	--
SJB-18-OA	.25	.00	13.92	6.05	2.40	.31	--
SJB-19-OA	---	---	---	3.16	1.56	.20	--

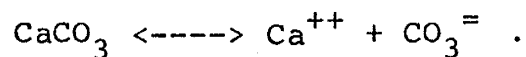
Table 5. Major ion concentrations in meq/l.

Sample #	Name	TAMERS	MOOK	VOGEL	PEARSON	FONTES
SJB-01-OA	Lybrook	43.5	80.1	85.0	84.6	68.5
SJB-02-OA	B of C Mission	41.4	92.7	85.0	81.9	69.5
SJB-03-OA	Pete Spring	51.6	-15.6	85.0	44.5	22.5
SJB-04-OA	Powerline WM	48.0	79.8	85.0	81.2	65.4
SJB-05-OA	Kimbeto WM	49.6	91.7	85.0	84.6	70.2
SJB-06-OA	Ojo Socorro	50.3	-43.1	85.0	31.6	10.5
SJB-08-OA	Dzilth	49.1	118.9	85.0	98.9	89.2
SJB-09-OA	Ojo Encino	55.4	-274.1	85.0	41.1	12.6
SJB-10-OA	Johnsons TP	45.9	95.4	85.0	83.2	70.3
SJB-11-OA	Huerfano #2	49.7	90.9	85.0	91.4	73.9
SJB-12-OA	Huerfano #1	46.2	92.5	85.0	79.8	69.3
SJB-13-OA	Nageezi CH	45.3	106.8	85.0	89.4	77.8
SJB-14-OA	Chaco Camp #9	50.5	84.5	85.0	89.4	71.7
SJB-15-OA	Hilltop	50.1	88.9	85.0	89.4	73.2
SJB-16-OA	Kah-Des-Pah	45.8	111.0	85.0	88.7	77.8
SJB-17-OA	Tsah Tah	47.1	82.2	85.0	75.1	63.2

Table 6. Initial ^{14}C activities (A_0) calculated using the five models.

where λ is the natural log of 2 divided by the ^{14}C half-life (5730 years); A is the measured radiocarbon activity of the water and A_0 is the initial activity calculated from the models.

Saturation indices for each water sample were calculated in order to determine the extent to which the water is supersaturated or undersaturated with respect to calcite. All but two samples (SJB-4-OA and SJB-9-OA) showed saturation indices greater than one for the following reaction:



This indicates that the water is supersaturated and the reaction will tend to the left. Dilution of the recharge zone initial ^{14}C activity by additional dead carbon should therefore not be a factor in calculating water ages.

Ages calculated using each of the five models are presented in Table 7. With the exception of Tamers' model, the ages seem to agree quite closely and consistently. The relatively young ages calculated using Tamers' model are most likely a reflection of the high pH values seen in the Ojo Alamo water. The measured $\delta^{13}\text{C}$ values (generally less than -14 ‰) indicate that a simple mixing approach (Tamers' model) is not adequate. If mineral and soil gas mixing were the only process, we would expect $\delta^{13}\text{C}$ values of -12.5 ‰ or less. The negative $\delta^{13}\text{C}$ is best explained by

Sample #	TAMERS	MOOK	VOGEL	PEARSON	FONTES	ERROR (yrs)
SJB-01-OA	15,200	20,300	20,800	20,700	19,000	+941/-842
SJB-02-OA	3,000	9,700	9,000	8,700	7,300	+249/-242
SJB-03-OA	modern	*****	900	modern	modern	+157/-155
SJB-04-OA	modern	3,700	4,200	3,800	2,000	+186/-182
SJB-05-OA	18,000	23,000	23,000	23,000	21,000	+1382/-1184
SJB-06-OA	modern	*****	3,000	modern	modern	+278/-269
SJB-08-OA	14,000	21,300	18,600	19,800	19,000	+872/-789
SJB-09-OA	modern	*****	modern	modern	modern	+183/-179
SJB-10-OA	modern	5,000	4,100	3,900	2,500	+161/-158
SJB-11-OA	20,000	24,000	24,000	25,000	23,000	+1129/-993
SJB-12-OA	19,000	25,000	24,000	24,000	23,000	+3446/-2425
SJB-13-OA	12,400	19,400	17,600	18,000	17,000	+469/-444
SJB-14-OA	11,000	15,300	15,300	15,700	13,900	+401/-383
SJB-15-OA	13,100	17,900	17,500	17,900	16,300	+629/-584
SJB-16-OA	21,000	29,000	26,000	27,000	26,000	+1845/-1507
SJB-17-OA	1,300	5,900	6,200	5,100	3,700	+187/-183

Table 7. Carbon-14 ages calculated according to the five models (rounded to the nearest 100 or 1000 years, depending on magnitude of error). *** indicates that the ages could not be determined due to negative initial activities.

isotopic exchange processes, and therefore the models which account for exchange processes are more appropriate than Tamers' model. Vogel's model results in ages very similar to those from Pearson's, Mook's and Fontes'. The fact that ages from Pearson's model agree so well with those from Mook's and Fontes' suggests that Pearson's model indirectly accounts for isotopic exchange by using an isotope balance of carbon-13 from different sources. Mook's model appears to overcorrect the young samples (3,6,9) resulting in a negative A_0 while it undercorrects some of the older samples (8,13,16) giving an initial activity above 100 pmc. The overcorrection arises from the model's assumption that isotopic exchange takes place in a closed system, which is not the case for the modern samples. Fontes and Garnier (1979) found that Mook's model was very sensitive to variations in $\delta^{13}\text{C}$. The extreme A_0 values calculated with this model most likely result from this sensitivity. The ages of old water calculated using Fontes' model are typically 10% younger than those calculated from Pearson's while young samples may be as much as 47% younger. However, these differences are not particularly significant relative to the age of the sample.

Ages calculated using Fontes model will be used subsequently in this report. This model is the most appropriate because it accounts for both the isotopic exchange processes and the carbonate reactions which occur within this aquifer, but does not exhibit the

oversensitivity of the Mook model. However, ages from all of the four models (omitting Tamers') are reasonably concordant, and thus the choice of any one in particular is relatively unimportant.

Figure 12 is an isochron map using ages from Fontes' model. It verifies the accuracy of the potentiometric surface map (Figure 5) by showing that flow perpendicular to the potentiometric lines increases in age with distance from outcrop. In addition, it shows variations of hydraulic conductivity within the aquifer, inferred from the differing water ages at similar distances from the outcrop.

A sensitivity analysis was run on Pearson's, Mook's and Fontes' models in order to test the accuracy of the assigned values for nonmeasured parameters. Values were varied to possible extremes and initial activities were calculated. Table 8 shows the results of the analysis. Although A_0 values differ, most permutations do not produce large variations in the calculated ages. Those which do give large age variations also have physically unrealistic initial activities, and may therefore be disregarded.

Tritium

Tritium analyses were performed on fifteen water samples. The results are presented in Table 9. Three of the samples have significant tritium concentrations with the remaining twelve samples at or near background. SJB-1-OA

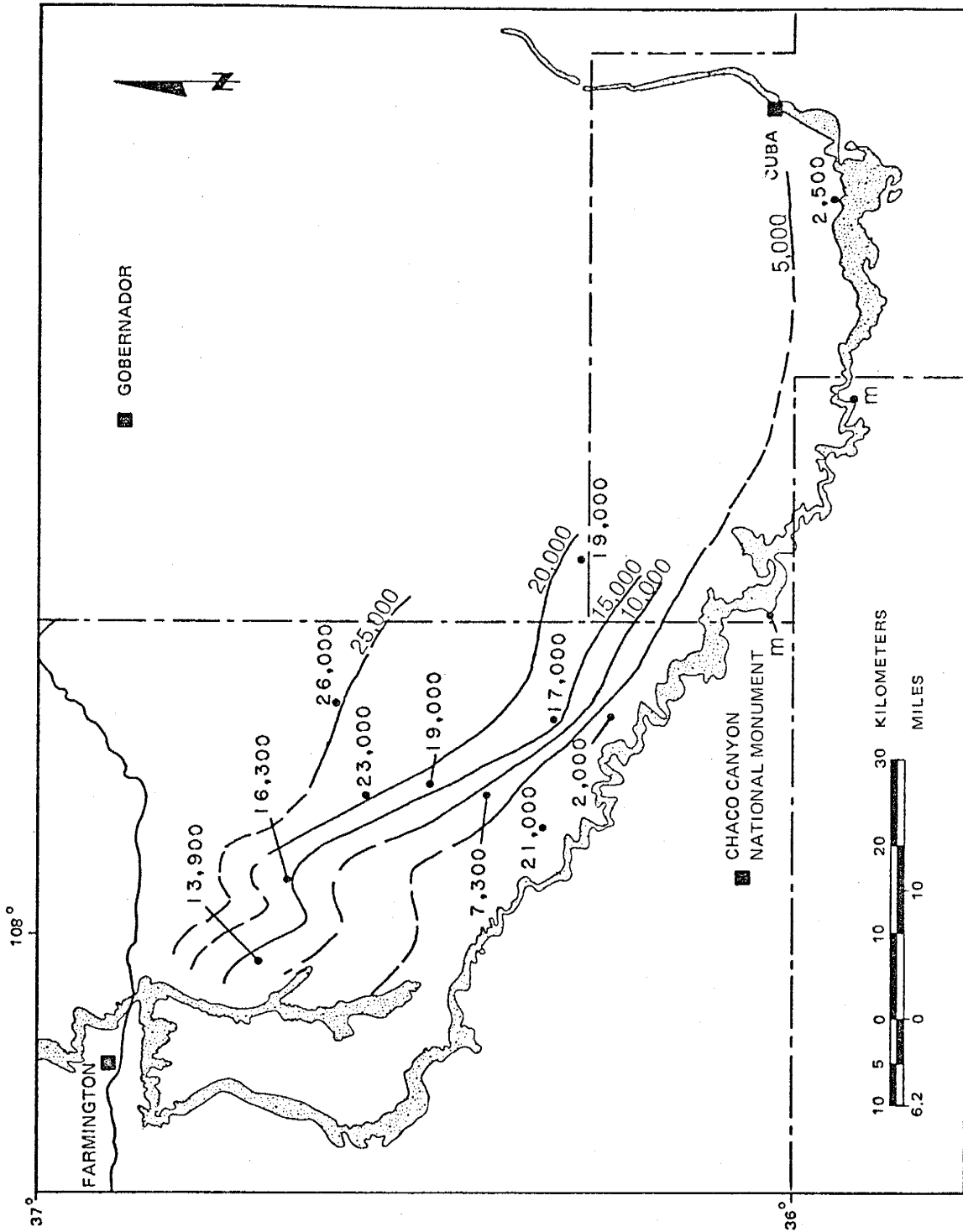


Figure 12. Map showing age of water in the Ojo Alamo aquifer according to Fontes' model. Isochrons drawn at 5000 year intervals.

	FONTES				MOOK				PEARSON			
	<u>SJB-1-OA</u>		<u>SJB-2-OA</u>		<u>SJB-1-OA</u>		<u>SJB-2-OA</u>		<u>SJB-1-OA</u>		<u>SJB-2-OA</u>	
	<u>Ao</u>	<u>Age</u>	<u>Ao</u>	<u>Age</u>	<u>Ao</u>	<u>Age</u>	<u>Ao</u>	<u>Age</u>	<u>Ao</u>	<u>Age</u>	<u>Ao</u>	<u>Age</u>
$\delta g, Ag, \delta m, Am$												
-20,100, 0, 0	99	22	104	11	-226	---	-68	---	127	24	123	12
-20,100,-2.8, 0	99	22	105	11	396	34	-410	---	137	25	131	13
-25,100, -1, 0	64	18	64	6.7	77	20	91	9.6	83	21	81	8.5
-25,100,-2.8, 0	58	18	59	5.9	70	19	86	9.1	81	20	77	8.2
-30,100, 0, 0	49	16	49	4.5	51	17	53	5.1	63	18	61	6.3
-25,103,-2.8, 5	62	18	62	6.4	73	20	89	9.4	84	21	81	8.6
-16,100, 0, 0	165	26	185	15	34	13	30	0.5	212	28	205	16
-16,100,-2.8, 0	219	29	281	19	34	13	30	0.5	309	31	296	19

Table 8. Results of a sensitivity analysis on Fontes', Mook's and Pearson's models. Initial activities are in pmc. Ages are reported in thousands of years and are rounded off to the nearest thousand years for ages older than 10,000 and to the nearest hundred years for ages less than 10,000. δg and δm are the carbon-13 concentrations (per mille versus PDB) for soil gas and mineral carbonate, respectively. Ag and Am are the radiocarbon activities (pmc) of the soil gas and mineral carbonate. --- indicates that the age could not be calculated due to a negative A_0 value.

Sample #	Name	TU	+/-
SJB-01-OA	Lybrook	-0.4	0.6
SJB-02-OA	B of C Mission	3.2	0.7
SJB-03-OA	Pete Spring	26.7	1.1
SJB-04-OA	Powerline WM	1.6	0.7
SJB-05-OA	Kimbeto WM	3.2	0.7
SJB-06-OA	Ojo Socorro	49.8	1.1
SJB-08-OA	Dzilh	1.7	0.6
SJB-09-OA	Ojo Encino	41.9	0.9
SJB-10-OA	Johnson's TP	2.7	0.7
SJB-11-OA	Huerfano #2	2.1	0.6
SJB-12-OA	Huerfano #1	0.8	0.6
SJB-13-OA	Nageezi CH	1.8	0.6
SJB-14-OA	Chaco Camp #9	1.5	0.8
SJB-15-OA	Hilltop	1.7	0.8
SJB-16-OA	Kah-Des-Pah	3.2	0.8

Table 9. Tritium concentrations in Tritium Units (TU).

was determined to have a tritium concentration of -0.4 TU. The negative value arises when the measured disintegrations are less than background levels. In this case, the tritium concentration can be considered zero.

Noble Gases

Triplicate samples at two locations were taken for noble gas analysis. At the time of this writing the analyses were not completed. Results and interpretation of the noble gas analyses will be included in the completion report for the continuation of this project, which will be issued in July 1984.

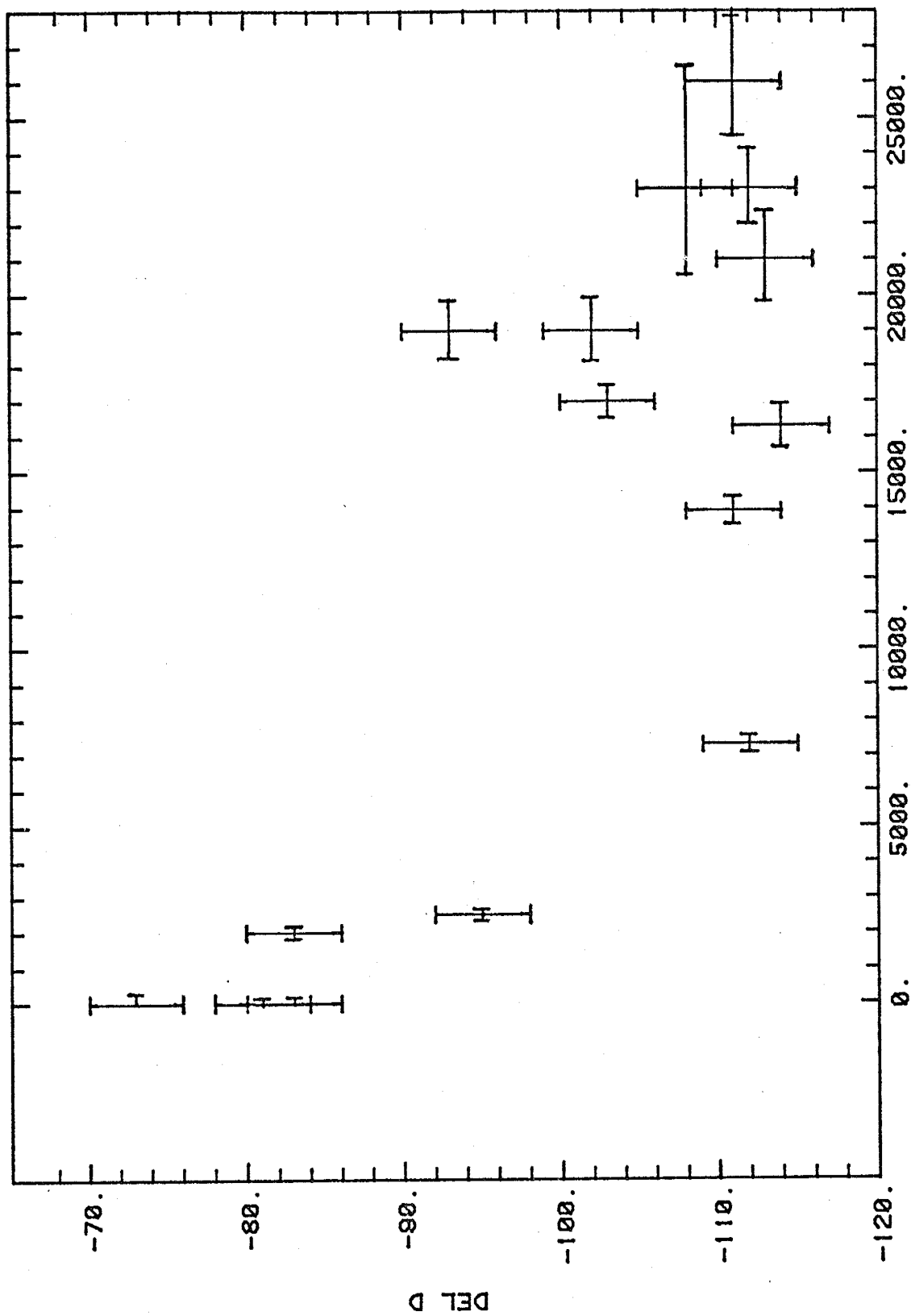
INTERPRETATION OF RESULTS

Stable Isotopes

Dansgaard (1964) demonstrated a clear correlation between precipitation temperature and the isotopic composition of the precipitation. This naturally led to the expectation that Pleistocene - Holocene temperature changes would be reflected in the isotopic composition of ground water. An idea of the magnitude of the isotopic shift was obtained when Pleistocene dated ice from Greenland showed a depletion in oxygen-18 of -13 ‰ (Dansgaard et al., 1969). Investigators have since looked for evidence of this shift in ground water, but a shift of the same magnitude has not yet been observed. Data have often been contradictory, leading to conflicting conclusions. However, studies in some parts of the world are now bringing forth a consistent pattern. Investigators in northern Africa and the Middle East (Gonfiantini et al., 1974a and 1974b; Sonntag et al., 1979; Gat and Dansgaard, 1972; Issar et al., 1972; Gat and Issar, 1974) have found a $\Delta\delta D$ ranging from -15 ‰ to -45 ‰ and a $\Delta\delta^{18}\text{O}$ of -2 ‰ to -4 ‰ . In western and central Europe investigators (Smith et al., 1976; Bath et al., 1979; Evans et al., 1979; Fontes and Garnier, 1979) have found that $\Delta\delta D$ ranges from -49 ‰ to -15 ‰ and the $\Delta\delta^{18}\text{O}$ varies between -0.7 ‰ and -1.5 ‰ . Studies from other geographical areas are scarce and the conclusions are often contradictory. In North America, it has been thought,

until recently, that there had been no isotopic shift in Pleistocene precipitation. Studies of aquifers in Texas, Florida, Nevada, California, the Atlantic Coastal Plains and the northern Great Plains (Hanshaw et al., 1978 and 1979) indicated no significant depletion in heavy isotopes for Pleistocene ground water. However, recent investigations (White, 1981; Siegel and Mardle, 1982; Fritz et al., 1974) have found evidence that support the idea of a large negative isotopic shift, although the Pleistocene age of these waters has not always been verified by carbon-14 analyses. Another technique, using the deuterium content of fluid inclusions in dated speleothems (Harmon et al., 1979a and 1979b; Harmon and Schwarcz, 1981) lends support to the hypothesis of lighter Pleistocene precipitation, although not as markedly lighter as the ground-water studies cited above. On the other hand, Epstein and Yapp (1976) and Yapp and Epstein (1982a) found that deuterium measurements of Pleistocene wood indicate that Pleistocene precipitation was significantly heavier than modern precipitation.

Stable isotope analyses of water from the Ojo Alamo Sandstone resulted in measured variations in δD of -114 ‰ to -73 ‰ and $\delta^{18}O$ from -15.6 ‰ to -7.1 ‰. These results, used in conjunction with the carbon-14 dates, suggest that Pleistocene recharge was isotopically lighter than modern-day recharge (Figure 13). There are several possible explanations for the anomalously light waters. Following is a discussion of each and its plausability.



AGE (CA)

Figure 13. A graphical comparison of δD and ^{14}C age.

(1) The isotopically light waters represent recharge from higher elevations. The magnitude of the elevation effect varies from place to place. Stahl et al. (1974) reported a change of $-12 \text{ }^{\circ}/\text{oo } \delta\text{D}/1000\text{m}$ in Greece while Niewodnicanski et al. (1981) determined a $-80 \text{ }^{\circ}/\text{oo } \delta\text{D}/1000\text{m}$ in the Andes Mountains. Although scarce, the available data (Goff et al., 1982) suggest that the elevation effect for New Mexico is about $-35 \text{ }^{\circ}/\text{oo } \delta\text{D}/1000\text{m}$. The maximum topographic relief of the study area is 400 meters which could only account for a $-14 \text{ }^{\circ}/\text{oo } \delta\text{D}$ shift. This change in elevation is clearly insufficient to explain the observed isotopic depletion.

(2) Preferential seasonal recharge due to differing vegetative cover. Fritz et al. (1974) account for a $30 \text{ }^{\circ}/\text{oo } \delta\text{D}$ variation in modern water in the Winnepeg, Canada area by considering the different vegetation covers in the recharge area. They found that recharge in forested areas was isotopically lighter than recharge in grasslands. This is due mainly to the higher summer moisture consumption of the forest vegetation. However, this explanation is not applicable to this project. The area under investigation is of fairly uniform vegetational cover. Sagebrush and grasses dominate the countryside, although pinyon and juniper are sparsely present at higher elevations. This slight variation in

vegetational cover could hardly account for the observed $\Delta\delta D$ and $\Delta\delta^{18}O$.

(3) The isotopically light water is the result of recharge at higher latitudes. This is not a likely explanation in as much as the recharge area barely spans one degree in latitude. In addition, the potentiometric map for the Ojo Alamo Sandstone indicates that the isotopically light water actually comes from lower latitude recharge areas.

(4) The isotopically depleted waters represent recharge during cooler climatic conditions. This is the most feasible explanation. The magnitude of the observed shift is on the order of -41 ‰ and about -5 ‰ for $\Delta\delta D$ and $\Delta\delta^{18}O$, respectively. Carbon-14 dating indicates that this isotopic change in precipitation has occurred over a 26,000 year period. This is in accordance with the hypothesized "Pleistocene shift".

As discussed above, Figure 13 implies that Pleistocene recharge was isotopically lighter than modern recharge. The combined effects of a cooler, wetter climate with a larger percentage of winter recharge and Pacific frontal storms as the principal moisture source most probably account for the isotopically depleted waters of Pleistocene age.

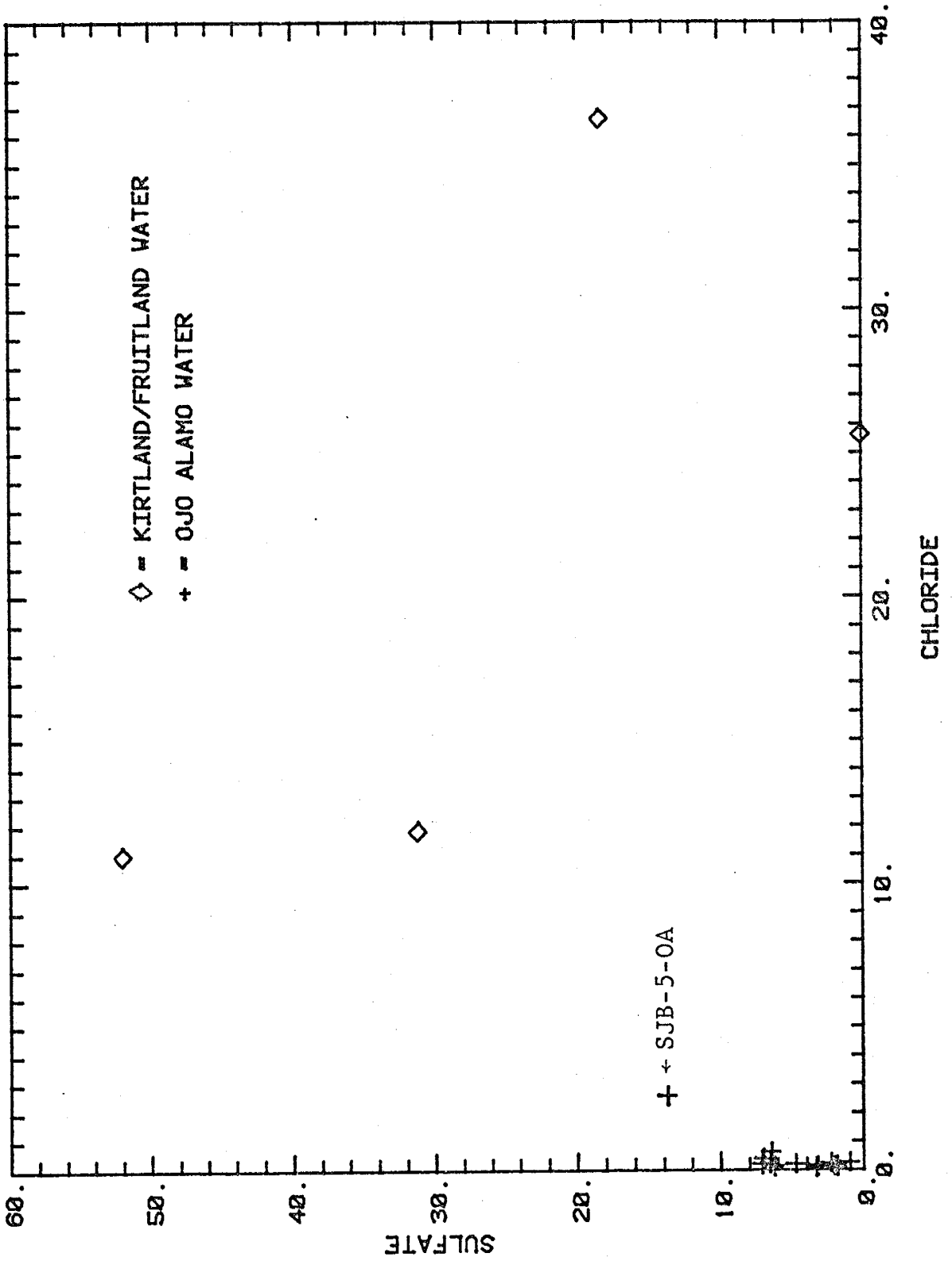
Carbon-14

Water from one well, SJB-5-OA, gives an anomalously high age compared to other nearby wells. An age of 21,000 years was calculated, and yet the well is located less than 2 km from the recharge area. This could possibly indicate an area of extremely low hydraulic conductivity. However, consideration of the chemical characteristics of the water from this well (Table 4) indicates that the water is probably not derived from the Ojo Alamo aquifer. In fact, on a graph of sulfate versus chloride for water from the Ojo Alamo Sandstone and the Kirtland/Fruitland Formation (Figure 14), SJB-5-OA plots between Kirtland/Fruitland and Ojo Alamo data points. This suggests that the well is probably not completed in the Ojo Alamo Sandstone, but rather is tapping the Kirtland Shale. The age determination for SJB-5-OA will therefore not be used in hydraulic conductivity calculations.

The isochron map (Figure 12) indicates that there are areas with differing hydraulic conductivities in the Ojo Alamo Sandstone. For example, the travel distance for a 15,000 year old sample in one area does not necessarily correspond to the same distance in another area.

Quantitative assesment of the varying hydraulic conductivities was accomplished using the equation:

$$K = (n*\Delta l^2) / (a*\Delta h)$$



where K is the hydraulic conductivity, n is the porosity, Δl is the distance traveled, a is the change in age over Δl , and Δh is the change in head over Δl . A porosity of 20% was determined in the laboratory and was assumed to be constant. Δl and Δh values were taken from the potentiometric map (Figure 5) and changes in age were figured from the ground-water age map (Figure 12). Hydraulic conductivities were calculated for each 50 meter head drop along a flow path.

Figure 15 shows the results of these calculations. Three zones of hydraulic conductivity can be delineated. Values range from less than 10^{-6} m/sec to greater than 10^{-5} m/sec. Brimhall (1973) reported the transmissivities for three wells in the study area (25.9.19.114; 27.12.13.142; 27.12.13.222) to be 1.5×10^{-4} m²/sec, 1.7×10^{-4} m²/sec, and 9.5×10^{-5} m²/sec. The aquifer thickness at these three locations is 22.4, 22.7 and 20.1 meters, respectively, which gives hydraulic conductivities of 5.1×10^{-6} m/sec, 7.4×10^{-6} m/sec, and 4.7×10^{-6} m/sec. All of these values fall within the proper hydraulic conductivity zones as determined in this report.

Tritium

Figure 16 shows tritium concentrations plotted against radiocarbon ages. A strong correlation is apparent. Those samples which gave carbon-14 dates of modern age

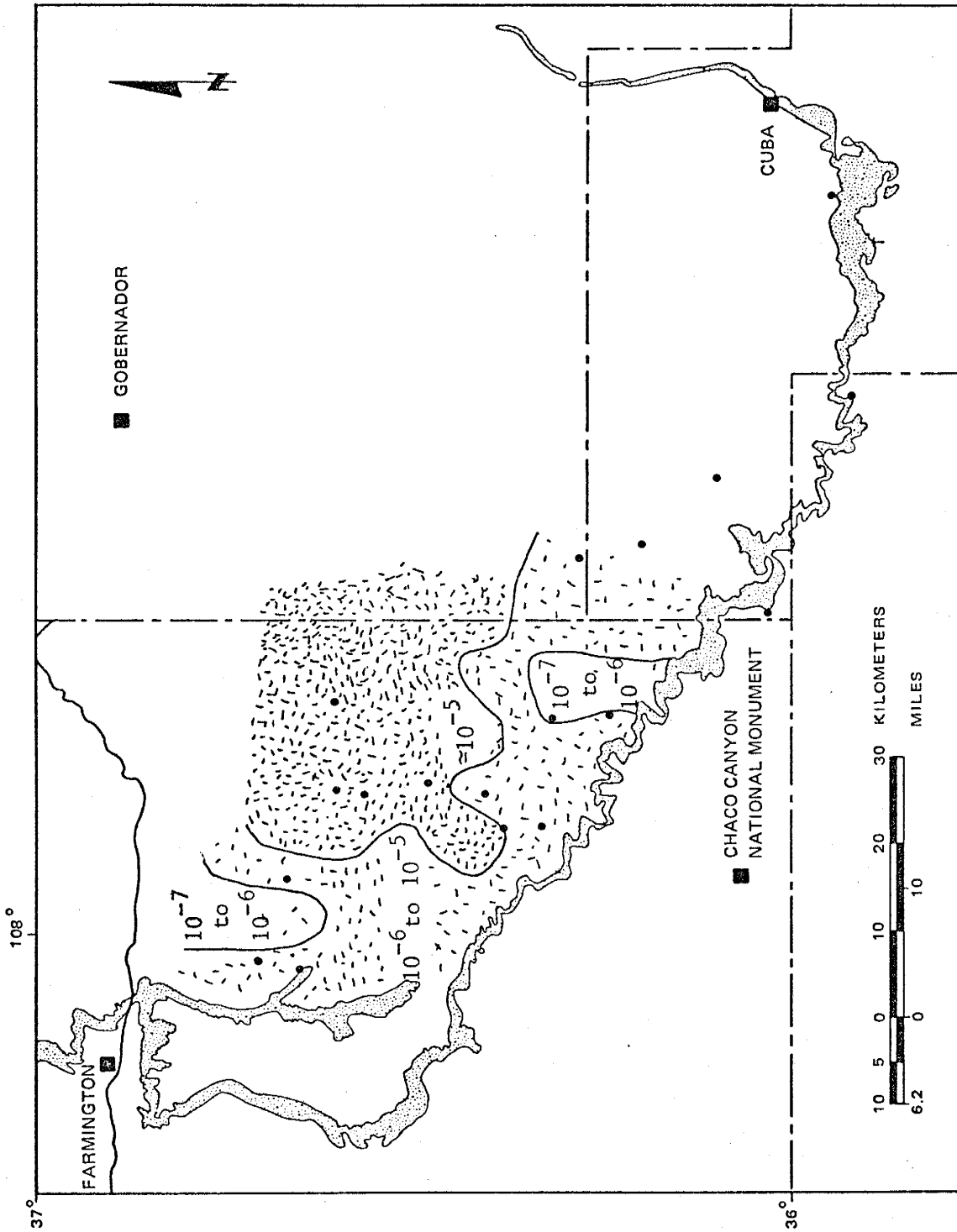
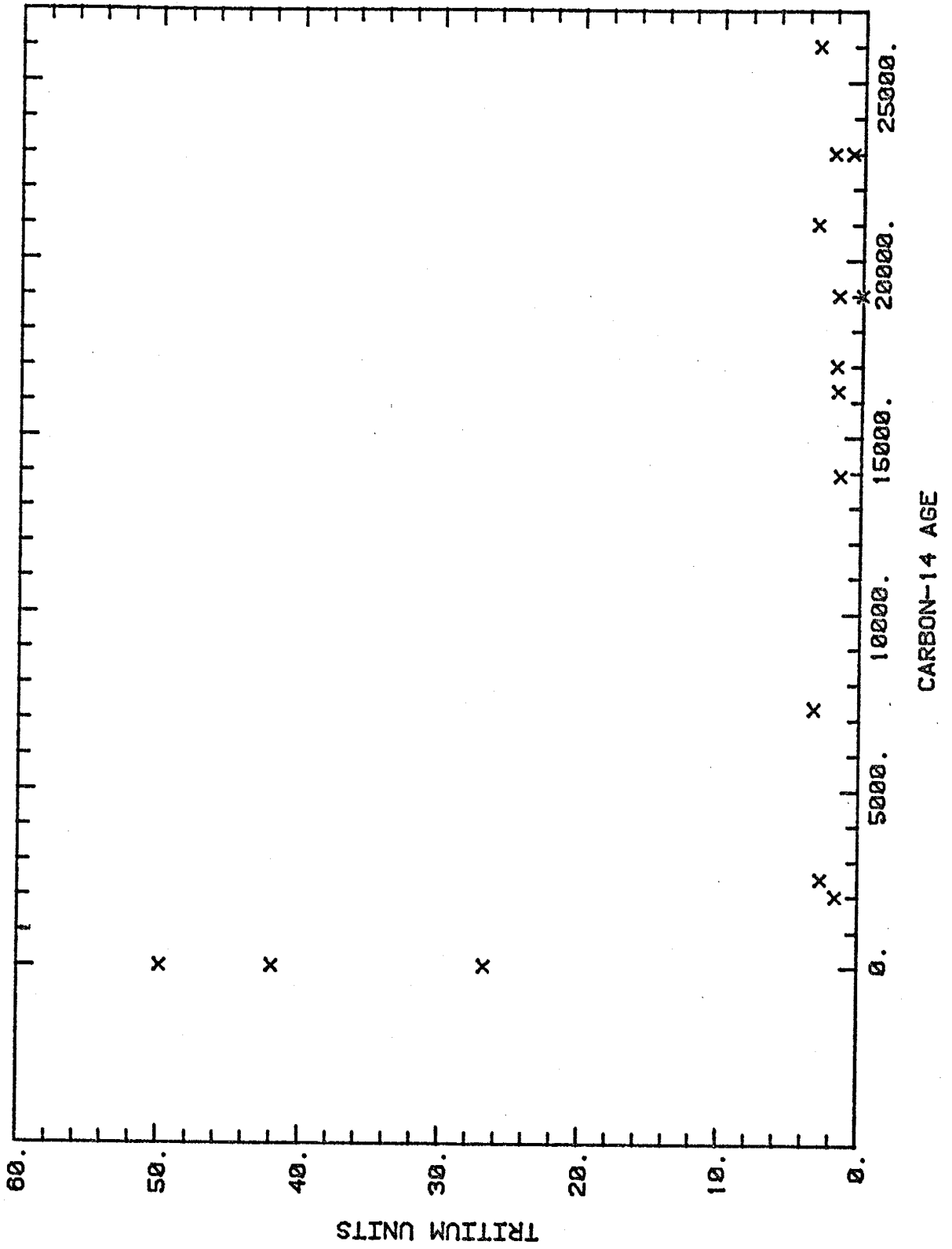


Figure 15. Hydraulic conductivities calculated from ^{14}C ages and potentiometric surface map (Figure 5).



(SJB-3,6,9,-OA) have tritium contents of 27, 50 and 42 TU. This suggests that (1) the water is very recent (present tritium concentrations in precipitation are between 40 and 50 TU) or (2) the water has both pre-bomb (before 1953) and post-bomb components. The presence of appreciable tritium in these three water samples indicates that modern precipitation is infiltrating and recharging the aquifer.

For those samples that were carbon-14 dated as older than modern, tritium concentrations are virtually negligible. This eliminates the possibility of recent (post-1953) water being present, although it does not exclude the possibility of very minor mixing with non-tritiated modern water (i.e., pre-1953 precipitation).

SUMMARY

A potentiometric surface map for the Ojo Alamo Sandstone was presented. Although head data for some parts of the study area are scarce, it was possible to construct a fairly detailed map for the aquifer in San Juan County. Ground-water flow is generally to the north-northwest and discharges where the San Juan River intersects the outcrop of the Ojo Alamo Sandstone. However, there is a north-northeast component to the flow regime and where these two flow patterns meet, south of Bloomfield, convergent flow phenomena can be expected. Vertical leakage into the Ojo Alamo Sandstone was considered. Examination of vertical head gradients between the Ojo Alamo and the overlying and underlying units indicated that over most of the study area the potential for downward leakage exists. Estimates of leakage rates using Darcy's Law suggest that water from the overlying Nacimiento Formation amounts to about 2% of the flow in the Ojo Alamo Sandstone.

Fifteen water samples were analysed for radiocarbon content. Ages were calculated using the models of Vogel, Tamers, Pearson, Mook and Fontes. Upon examination of water chemistry and carbon isotope data, Fontes' model was determined to be the most appropriate and these ages were used for hydraulic conductivity estimates. The oldest water sampled was 26,000 years. Three different zones of hydraulic conductivity were outlined. Values ranged from

3×10^{-7} m/sec to 10^{-5} m/sec. The reliability of these zones is substantiated by three hydraulic conductivity values determined from previous pump tests.

Tritium analyses of water from three springs, radiocarbon dated as modern, showed significant concentrations of tritium. This signifies that post-bomb (after 1953) precipitation is present in the spring water. These areas are therefore ones of active recharge.

Stable isotope analyses were performed on eighteen water samples. A strong correlation exists between isotopically depleted water and radiocarbon ages greater than 10,000 years. This correlation lends support to the hypothesis of a "Pleistocene shift" in North America. Until recently, few ground-water investigations have presented results that substantiate the idea of an isotopic shift in North American Pleistocene precipitation, although in other parts of the world it has been observed. These results are the first evidence that Pleistocene recharge in the southwest United States was isotopically lighter than modern recharge. This observation sheds light on the controversial subject of Pleistocene climatic conditions in the southwest. The depletion in deuterium and oxygen-18 of Pleistocene precipitation was most likely due to the combined effects of (1) a wetter climate (2) cooler temperatures (3) more winter recharge and (4) the principal source of moisture being the Pacific Ocean.

SIGNIFICANCE AND RECOMMENDATIONS

The significance of this study is twofold. First, it demonstrates the importance of the Tertiary aquifers in the San Juan Basin. The ground water is, in itself, a valuable resource, aside from its use for energy development. As with any resource, quantity, quality and availability should be known so that rational exploitation and informed regulation can occur. This study has laid the foundation for future isotopic ground-water investigations on the Tertiary aquifers of the basin. In a further effort to understand the three-dimensional flow system of the Tertiary units, a continuation of this study at New Mexico Institute of Mining and Technology, funded by New Mexico Water Resources Research Institute, is concentrating on the overlying Nacimiento and San Jose Formations. It is hoped that, in conjunction, these two studies will provide an understanding of the three-dimensional flow system, therefore allowing accurate numerical simulation of the ground-water resources.

Secondly, this study has contributed to the understanding of Pleistocene climate. Although the isotopic composition of Pleistocene-age ground water can reveal much about climatic conditions at that time, few data have been available. The results of this investigation provide a firm and reliable source of information on Pleistocene

precipitation in the southwest United States. Future isotopic studies might include (1) better establishing the meteoric water line for northwestern New Mexico (2) determining the elevation effect for the central San Juan Basin and (3) determining non-measured carbon-14 parameters.

REFERENCES

- Anderholm, S.K. (1979). Hydrogeology and water resources of the Cuba quadrangle, Sandoval and Rio Arriba Counties, New Mexico: New Mexico Institute of Mining and Technology, M.S. Thesis.
- Bailey, V. (1913). Life zones and crop zones of New Mexico: U.S. Department of Agriculture, North American Fauna, No. 35, 100 p.
- Baltz, E.H., Jr. (1967). Stratigraphy and regional tectonic implications of part of the Upper Cretaceous and Tertiary rocks, east-central San Juan Basin, New Mexico: U.S. Geol. Surv. Prof. Paper 552.
- Baltz, E.H., Jr.; Ash, S.R.; and Anderson, R.Y. (1966). History of nomenclature and stratigraphy of rocks adjacent to the Cretaceous - Tertiary boundary, western San Juan Basin, New Mexico: U.S. Geological Survey, Prof. Paper 524-D, 23p.
- Baltz, E.H., Jr.; and West, S.W. (1967). Ground-water resources of the southern part of the Jicarilla Apache Indian Reservation and adjacent areas, New Mexico: U.S. Geol. Surv., Water Supply Paper 1576-H.
- Bath, A.H.; Edmunds, W.M.; and Andrews, J.N. (1979). Paleoclimatic trends deduced from the hydrochemistry of a Triassic sandstone aquifer, United Kingdom: Isot. Hydrol., Proc. Int. Symp., 1978, IAEA, 2, 545-581.
- Bauer, C.M. (1916). Stratigraphy of a part of the Chaco River valley: U.S. Geol. Surv., Prof. Paper 98P, 271-278.
- Berry, F.A.F. (1959). Hydrodynamics and geochemistry of the Jurassic and Cretaceous Systems in the San Juan Basin, northwestern New Mexico and southwestern Colorado: Stanford University, Ph.D. Dissertation.
- Bigeleisen, J. (1952). The effects of isotopic substitutions on the rates of chemical reactions: J. Phys. Chem., 56, 823-828.
- Brimhall, R.M. (1973). Ground water hydrology of Tertiary rocks of the San Juan Basin, New Mexico: Four Corners Geological Society Memoir, p.197-207.
- Brown, B. (1910). The Cretaceous Ojo Alamo beds of New Mexico, with description of the new dinosaur genus Kritosaurus: American Museum of Natural History, Bull., 28, 267-274.

- Brown, D.R. (1976). Hydrogeology and water resources of the Aztec quadrangle, San Juan County, New Mexico: M.S. thesis, New Mexico Institute of Mining and Technology, 174 p.
- Bushman, F.X.; and Foster, R. (1957). Ground-water conditions at Cuba independent rural schools new well site: unpublished New Mexico Bureau of Mines and Mineral Resources Report, 15p.
- Cooley, M.E.; Harshbarger, J.W.; Akers, J.P.; and Hardt, W.F. (1969). Regional hydrogeology of the Navajo and Hopi Indian Reservations: U.S. Geol. Surv. Prof. Paper 521-A.
- Cooper, J.B.; and John, E.C. (1968). Geology and ground water occurrence in southeastern McKinley County, New Mexico: New Mexico State Engineer Technical Report 35.
- Cooper, J.B.; and Trauger, F.D. (1967). San Juan River basin - geography, geology, and hydrology, in Water Resources of New Mexico-Occurrence, Development and Use: New Mexico State Planning Office, 185-210.
- Craig, H. (1954). Carbon-13 in plants and the relationship between carbon-13 and carbon-14 variations in nature: J. Geol., 62, 115-149.
- Craig, H. (1961b). Isotopic variations in meteoric water: Science, 133, 1702-1703.
- Craig, S.E. (1980). Hydrogeology and water resources of the Chico Arroyo-Torreon Wash area, McKinley and Sandoval Counties, New Mexico: M.S. Thesis, New Mexico Institute of Mining and Technology.
- Dane, C.H. (1946). Stratigraphic relations of Eocene, Paleocene, and latest Cretaceous formations of the eastern side of San Juan Basin, New Mexico: U.S. Geol. Survey, Oil and Gas Investigations Preliminary Chart 24.
- Dansgaard, W. (1964). Stable isotopes in precipitation: Tellus, 16, 436-468.
- Dansgaard, W.; Johnsen, S.J.; Moeller, J.; and Langway, C.C., Jr. (1969). One thousand centuries of climatic record from Camp Century on the Greenland ice sheet: Science, 166, 377-381.
- Epstein, S.; and Mayeda, T. (1953). Variations of the oxygen-18 content of waters from natural sources: Geochim. Cosmochim. Acta, 4, 213-224.

- Epstein, S.; and Yapp, C.J. (1976). Climatic implications of the D/H ratio of hydrogen in C-H groups in tree cellulose: Earth Planet. Sci. Lett., 30, 252-261.
- Epstein, S.; and Yapp, C.J. (1977). Climatic implications of D/H ratios of meteoric water over North America (9500-22000 B.P.) as inferred from ancient wood cellulose C-H hydrogen: Earth and Planet. Sci. Lett., 34, 333-350.
- Evans, G.V.; Otlet, R.L.; Downing, R.A.; Monkhouse, R.A.; and Rae, G. (1979). Some problems in the interpretation of isotope measurements in United Kingdom aquifers: Isotope Hydrology 1978, Proc. Int. Symp., IAEA, Vienna, 2, 679-708.
- Fassett, J.E. (1973). The Saga of the Ojo Alamo Sandstone; or the Rock-stratigrapher and the Paleontologist should be Friends: Four Corners Geological Society Memoir.
- Fassett, J.E.; and Hinds, J.S. (1971). Geology and fuel resources of the Fruitland Formation and Kirtland Shale of the San Juan Basin, New Mexico and Colorado: U.S. Geol. Surv. Prof. Paper 676.
- Faure, G. (1977): Principles of Isotope Geology: Wiley, New York, N.Y., 464 p.
- Fontes, J.CH. (1980). Environmental isotopes in groundwater hydrology: Handbook of Environmental Isotope Geochemistry (Fritz, P.; and Fontes, J.Ch., eds.), 1, 75-140.
- Fontes, J.CH.; and Garnier, J.M. (1979). Determination of the initial C-14 activity of the total dissolved carbon - A review of the existing models and a new approach: Water Resour. Research., 15, 399-413.
- Freeze, A.F.; and Cherry, J.A. (1979). Groundwater: Prentice-Hall, Inc., New Jersey.
- Fritz, P.; Drimmie, R.J.; and Render, F.W. (1974). Stable isotope contents of a major prairie aquifer in central Manitoba, Canada: Isot. Tech. in Groundwater Hydrol., 1974, Proc. IAEA Symp., Vienna, 1, 379-398.
- Gat, J.R. (1980). The isotopes of hydrogen and oxygen in precipitation: Handbook of Environmental Isotope Geochemistry (Fritz, P.; and Fontes, J.Ch., eds.), 1, 21-47.
- Gat, J.R.; and Carmi, I. (1970). Evolution of the isotopic composition of atmospheric waters in the Mediterranean Sea area: J. Geophys. Res., 75, 3039-3048.
- Gat, J.R.; and Dansgaard, W. (1972). Stable isotope survey of the fresh water occurrences in Israel and the northern Jordan Rift Valley: J. Hydrol., 16, 177-212.

- Gat, J.R.; and Issar, A. (1974). Desert isotope hydrology: Water sources of the Sinai Desert: Geochim. Cosmochim. Acta, 38, 1117-1131.
- Goff, F.; McCormick, T.; Gardner, J.N.; Trujillo, P.E.; Counce, D.; Vidale, R.; and Charles, R. (1982). Water geochemistry of the Lucero Uplift, New Mexico - A geothermal investigation of low-temperature mineralized fluids: Los Alamos National Laboratory Report LA-9738-OBES.
- Gonfiantini, R.; Conrad, G.; Fontes, J.C.; Sauzy, G.; and Payne, B.R. (1974a). Etude isotopique de la nappe du Continental Intercalaire et de ses relations avec les autres nappes du Sahara septentrional: Isot. Tech. in Groundwater Hydrol., 1974, Proc. IAEA. Symp., Vienna, 1, 227-292.
- Gonfiantini, R.; Dincer, T.; and Derekoy, A.M. (1974b). Environmental isotope hydrology in the Hodna Region, Algeria: Isot. Tech. in Groundwater Hydrol., 1974, Proc. IAEA Symp., Vienna, 1, 293-316.
- Hanshaw, B.B.; Pearson, F.J.; and Winograd, I.J. (1978). Deuterium and oxygen-18 content of Holocene through late Wisconsin precipitation: Geol. Soc. Am., Abstr. Prog., 10, 415-416.
- Hanshaw, B.B.; Winograd, I.J.; and Pearson, F.J., Jr. (1979). Stable isotopes of subglacially precipitated carbonates and of ancient groundwaters. - Paleoclimatic implications: Proc. Int. Meeting on Stable Isotopes in Tree Ring Research, New Paltz, New York, May 22-25.
- Harmon, R.S.; and Schwarcz, H.P. (1981). Changes of deuterium and oxygen-18 enrichment of meteoric water and Pleistocene glaciation: Nature, 290, 125-128.
- Harmon, R.S.; Schwarcz, H.P.; Ford, D.C.; and Koch, D.L. (1979a). An isotopic paleotemperature record for late Wisconsinan time in northeast Iowa: Geology, 7, 430-433.
- Harmon, R.S.; Schwarcz, H.P.; and O'Neil, J.R.; (1979b). D/H ratios in speleothem fluid inclusions - A guide to variations in the isotopic composition of meteoric precipitation?: Earth Planet. Sci. Lett., 42, 254-266.
- IAEA, 1973. Environmental Isotope Data, 4. World Survey of Isotope Concentration in Precipitation (1968-1969). IAEA Tech. Rep. Ser., 147, 334p.
- Ingerson, C.W.; and Pearson, F.J. (1964). Recent Research in the Field of Hydrosphere, Atmosphere, and Nuclear Geochemistry: Sugawara Festival Volume, Maruzen Co., Japan, 263-283.

- Issar, A.; Bein, A.; and Michaeli, A. (1972). On the ancient water of the Upper Nubian sandstone aquifer in central Sinai and southern Israel: J. Hydrol., 17, 353-374.
- Kelley, V.C. (1950). Regional structure of the San Juan Basin: New Mexico Geological Society, Guidebook 1st field conference, 101-108.
- Keyes, C.R. (1906). Geological section of New Mexico: Science, new series, 23, 921-922.
- Kottlowski, F.E. (1975). Report of the Coal Resources Committee: State of New Mexico, Governor's Energy Task Force, 44p.
- Libby, W.F. (1955). Radiocarbon Dating: University of Chicago Press, Chicago, Ill.
- Lyford, F.P. (1979). Ground Water in the San Juan Basin, New Mexico and Colorado: U.S. Geol. Surv., Water-resources Investigations 79-73.
- Mazor, E. and Fournier, R.O. (1972). More on noble gases in Yellowstone National Park hot waters: Geochim. Cosmochim. Acta, 37, 515-525.
- Mazor, E. and Wasserburg, G.J. (1965). Helium, neon, argon, krypton and xenon in gas emanations from Lassen Volcanic and Yellowstone National Parks: Geochim. Cosmochim. Acta, 29, 443-454.
- McDonald, R.E. (1972). Eocene and Paleocene rocks of the southern and central basins: Geological Atlas of the Rocky Mountain Region, United States of America (Mallory, W.W., ed.), Rocky Mountain Assoc. of Geologists, Denver, 243-256.
- Mook, W.G. (1972a). On the reconstruction of the initial C-14 content of ground water from chemical and isotopic composition: Proc. VII Int. Conf. on C-14, Lower Hutt, New Zealand, October, 1972, PD-31, 18-25.
- Mook, W.G. (1976). The dissolution-exchange model for dating groundwater with carbon-14: Interpretation of Environmental Isotope and Hydrochemical Data in Groundwater Hydrology, IAEA, Vienna, 213-225.
- Mook, W.G. (1980). Carbon-14 in hydrogeological studies: Handbook of Environmental Isotope Geochemistry (Fritz, P.; and Fontes, J.Ch., eds.), 1, 49-74.
- Munnich, K.O. (1957). Messungen des 14-C Gehaltes vom hartem Grundwasser: Naturwiss., 44, p. 32.

- Munnich, K.O.; Roether, W.; and Thilo, L. (1967). Dating of ground water with tritium and 14-C: Isotopes in Hydrology, IAEA, Vienna, 305-319.
- Niewodniczanski, J.; Grabezak, J.; Baranski, L.; and Rzepka, J. (1981). The altitude effect on the isotopic composition of snow in high mountains: J. Glaciol., 27, 99-111.
- O'Sullivan, R.B.; and Beikman, H.M. (1963). Geology, structure, and uranium deposits of the Shiprock quadrangle, New Mexico and Arizona: U.S. Geological Survey, Miscellaneous Geological Investigations Map I-345, scale 1:24,000.
- Phillips, F.M. (1981). Noble Gases in Ground Water as Paleoclimatic Indicators: Univ. of Ariz., Ph.D. Dissertation.
- Rapp (1959). Reconnaissance of the geology and ground water resources of the Farmington area, San Juan County, New Mexico: U.S. Geol. Surv., Openfile Report SJ-7.
- Reeside, J.B., Jr. (1924). Upper Cretaceous and Tertiary formations of the western part of the San Juan Basin, Colorado and New Mexico: U.S. Geol. Surv. Prof. Paper 134.
- Renick, B.C. (1931). Geology and ground water resources of western Sandoval County, New Mexico: U.S. Geol. Surv. Water Supply Paper 525-C.
- Shomaker, J.W.; Beaumont, E.C.; and Kottowski, F.E. (1971). Strippable low-sulfur coal resources of the San Juan Basin in New Mexico and Colorado: New Mexico Bureau of Mines and Mineral Resources, Mem. 25, 189 p.
- Shomaker, J.W.; and Stone, W.J. (1976). Availability of ground water for coal development, San Juan Basin, New Mexico: Guidebook to Coal Geology of northwest New Mexico (Beaumont, E.C.; Shomaker, J.W.; and Stone, W.J., eds.), Mexico Bureau of Mines and Mineral Resources, Circular 154, 43-48.
- Siegel, D.I.; and Mardle, R.J. (1982). Geochemical evidence for Pleistocene glacial meltwater recharge to the Cambrian-Ordovician aquifer in the north-central United States: EOS, 63, 325-326.
- Simpson, G.G. (1948). The Eocene of the San Juan Basin, New Mexico: Am. J. Science, 246, part 1, 257-282; part 2, 363-385.
- Sinclair, W.J.; and Granger, W. (1914). Paleocene deposits of the San Juan Basin, New Mexico: American Museum of Natural History, Bulle., 33, 297-316.

- Smith, D.B.; Downing, R.A.; Monkhouse, R.A.; Otlet, R.L.; and Pearson, F.J. (1976). The age of groundwater in the Chalk of the London Basin: Water Resour. Res., 12, 392-404.
- Sonntag, C.; Klitzsch, E.; Lohnert, E.P.; El-Shazly, E.M.; Muennich, K.O.; Junghans, C.; Thorweihe, U.; Weistroffer, K.; and Suailem, F.M. (1979). Paleoclimatic information from deuterium and oxygen-18 in carbon-14 dated north Saharian groundwaters: Isot. Hydrol., Proc. Int. Symp. 1978, IAEA, 2, 569-581.
- Stahl, W.; Aust, H.; and Donnas, A. (1974). Origin of artesian and thermal waters determined by oxygen, hydrogen, and carbon isotope analyses of water samples from the Sperkhios Valley, Greece: Isot. Tech. in Groundwater Hydrol., Proc. IAEA Symp., Vienna, 1, 317-339.
- Stone, W.J. (1979c). Water - key to energy production, northwest New Mexico, USA: Third World Congress on Water Resources, Mexico City, Proc., 2, 868-877.
- Stone, W.J.; Lyford, F.P.; Frenzel, P.F.; Mizell, N.H.; and Padgett, E.T. (1983). Hydrogeology and Water Resources of San Juan Basin, New Mexico: New Mexico Bureau of Mines and Mineral Resources, Hydrologic Report 6, 70 p.
- Suess, H.E. (1955). Radiocarbon concentrations in modern wood: Science, 122, 415-417.
- Sugisaki, R. (1961). Measurement of effective flow velocity of ground water by means of dissolved gases: Am. J. Sci., 259, 144-153.
- Tamers, M.A. (1967). Surface-water infiltration and groundwater movement in arid zones of Venezuela: Isot. in Hydrol., IAEA, Vienna, 339-351.
- Tamers, M.A. (1975). Validity of radiocarbon dates on groundwater: Geophys. Surv., 2, 217-239.
- Thilo, L.; and Munnich, K.O. (1970). Reliability of carbon-14 dating of ground water: effect of carbonate exchange: Isotopes in Hydrology, IAEA, Vienna, 259-269.
- van der Merwe, N.J. (1982). Carbon Isotopes, Photosynthesis, and Archaeology: Amer. Sci., 70, 596-606.
- Vogel, J.C. (1967). Investigation of groundwater flow with radiocarbon: Isotopes in Hydrology, IAEA, Vienna, 355-368.
- Vogel, J.C. (1970). Carbon-14 dating of groundwater: Isotope Hydrology 1970, IAEA, Vienna, 235-237.

- Vogel, J.C.; and Ehhalt, D. (1963). The use of carbon isotopes in ground water studies: Radioisotopes in Hydrology, IAEA, Vienna, 383-396.
- White, A.F. (1981). Controls on isotopic compositions of ground water systems in southern Nevada: EOS, 62, 286.
- Yapp, C.J.; and Epstein, S. (1982a). Climatic significance of the hydrogen isotope ratios in tree cellulose: Nature, 297, 636-639.

APPENDIX I

<u>MULTIPLY METRIC UNITS</u>	<u>BY</u>	<u>TO OBTAIN ENGLISH UNITS</u>
hectares	2.47	acres
cubic meters (m ³)	35.3	cubic feet (ft ³)
meters (m)	3.28	feet (ft)
meters/sec (m/sec)	3.28	feet/sec (ft/sec)
sq meters/day (m ² /day)	10.8	sq feet/day (ft ² /day)
cubic meters (m ³)	264.2	gallons
cubic meters/day (m ³ /day)	.183	gallons/minute (gpm)
centimeters (cm)	.39	inches (in)
kilometers (km)	.621	miles
sq kilometers (km ²)	.383	sq miles (mi ²)
metric ton	1.10	ton (net)

APPENDIX II

Procedure for sampling of water for carbon-14 analysis

- 1) Fill a 50 liter carboy with water leaving room for additional reagents. Do not let the water sample come in contact with the atmosphere and avoid introducing extraneous material.
- 2) Add some sample water to a vial containing 5 grams of ferrous sulfate and shake. Add to sample container and mix thoroughly.
- 3) Add 0.5 liter of saturated barium chloride solution and mix thoroughly.
- 4) Add enough "carbonate free" sodium hydroxide solution to bring the pH of the water sample above 8.
- 5) Add 40 ml of Percol 156, and stir rapidly.
- 6) Allow barium carbonate to precipitate out.
- 7) Add an additional amount of barium chloride to water sample to ensure complete precipitation. If the solution shows any cloudiness, add more barium chloride.
- 8) After all the barium carbonate has settled to the bottom, carefully decant off the water sample. Pour the precipitate into container and cap tightly. Seal with molten wax and label.
- 9) Rinse out the carboy with sample water and 1 N HCl.